2008

Development of an RNA aptamer to PD173955N through SELEX

Samir Mehanovic
Iowa State University

Development of an RNA aptamer to PD173955N through SELEX

by

Samir Mehanovic

A thesis submitted to the graduate faculty

in partial fulfillment of the requirements for the degree of

MASTER OF SCIENCE

Major: Biochemistry

Program of Study Committee:
Marit Nilsen-Hamilton, Major Professor
Amy Andreotti
W. Allen Miller

Iowa State University

Ames, Iowa

2008

To my dearest aunt who is always in my thoughts and my heart

TABLE OF CONTENTS

LIST OF FIGURES

LIST OF TABLES

ABSTRACT

With all the technology available to us, the causes of cancers are still puzzling researchers all over the world. Everyday different approaches are being tested to help cure various cancers. With the development of molecular biology, we are able to understand cancer more at molecular level, which helps us look at different methods to treat cancer patients.

The molecular basis for leukemia cancers are understood to a level where we are able to design treatments that specifically target proteins responsible for the disease. One of those proteins is the Bcr-Abl tyrosine kinase which is mostly responsible for chronic myelogenous leukemia. PD173955 is a drug that is capable of inhibiting Bcr-Abl tyrosine kinase more potently than any other chemotherapeutic drug reported drug. The problem with PD173955 and a very large number of other drugs is their limited solubility in aqueous environments which makes them less desirable for medical applications.

Aptamers are newly developed reagents and their utilization in medicinal applications is so far very limited. However their characteristics make them perfect tools to help solve problems associated with PD173955. Here we report a successful selection of the RNA aptamer that is capable of binding PD173955 with a dissociation constant of 1-2 μM using SELEX. The data obtained with selected aptamer suggests that the aptamer could be used to protect PD173955 from aqueous environment. The selection process of the RNA aptamer will be described in detail. The selected aptamer has been reduced to its minimal binding domain without loss of affinity.

CHAPTER 1: INTRODUCTION TO LEUKEMIA AND PROBLEMS ASSOCIATED WITH CURRENT TREATMENTS

INTRODUCTION

Leukemia

Leukemia is a type of cancer that affects cells in the blood and bone marrow, and results in overproduction of white blood cells. These abnormal cells are not capable of developing further and accumulate over time to displace normal blood cells. Based on how quickly leukemia advances, it is characterized into two types, chronic and acute. Chronic type leukemia progresses very slowly. An acute type of leukemia is more aggressive and progresses much faster. In addition to these two classifications, leukemia is also classified by the types of white blood cells that it influences.

There are four categories of leukemia. Chronic myeloid leukemia (chronic myelogenous leukemia, CML), accounts for about 4,600 new cases and 490 deaths in the U.S. each year. (Society 2007) It influences mainly adults. Chronic lymphocytic leukemia (chronic lymphoblastic leukemia, CLL), accounts for about 9,700 new cases in the U.S. each year. (Society 2007) Mostly it influences patients 55 or older. Acute myeloid leukemia (acute myelogenous leukemia, AML) accounts for about 11,900 new cases each year in the U.S. (Society 2007) It influences both adults and children. Acute lymphoblastic leukemia (acute lymphoblastic leukemia,

ALL) accounts for 4,000 new cases in the U.S. each year (Society 2007). It mostly influences children, but can influence adults.

CML affects the developmental pathway of white blood cells, called granulocytes, in the blood and bone marrow. Some of these cells never become mature white blood cells, and are called blasts. Over time, in people with CML granulocytes and blasts take over the blood cell population and displace red blood cells and platelets.

Depending on the number of blasts and granulocytes, there are three phases of leukemia. In the chronic phase, which is characterized as a slowly progressing disease, patients may have no leukemic symptoms. Most of the white blood cells are mature cells in the blood and bone marrow. The chronic phase can last from several months to several years, averaging about five years. In the accelerated phase of CML patients show symptoms of leukemia, which include fever, poor appetite, and weight loss. There are some immature white blood cells present in blood and bone marrow (between 5 to 30 percent) (Talpaz, Silver et al. 2002). In the blast crisis phase there are more then 30 percent immature white blood cells present in blood and bone marrow. Symptoms such as anemia and recurring infections are typical. Generally patients in the blast crisis phase of CML die within 6-12 months after being classified in this phase (Kurzrock, Kantarjian et al. 2003). The facts and statistics cited above regarding the nature of the leukemia and its statistics were obtained from http://www.leukemia-lymphoma.org/, and http://www.cancer.gov/, an official webpage of United States National Cancer Institute.

CML accounts for 20 percent of newly diagnosed leukemia cases in adults. If left untreated 20-30 percent of CML patients die within two years, and 25 percent die each subsequent year.

The causes of leukemia are still puzzling scientists and physicians, but studies identified certain factors that can contribute to development of the disease. For example, people who are exposed to high levels of radiation have a higher risk of developing leukemia then others. Such high levels of radiation are caused by atomic bombs or nuclear power plant accidents (such as Chernobyl in 1986). Medical treatments that use high levels of radiation to treat cancers, can be linked to the development of radiation-induced leukemia (Shuryak, Sachs et al. 2006). There is strong clinical and epidemiological evidence that ionizing radiation can cause leukemia by creating DNA damage. When hematopoietic cell lines were exposed to high levels of γ-irradiation, the formation of the fusion genes characterized in leukemia was observed (Deininger, Bose et al. 1998)

People who are exposed to certain chemicals such as benzene or formaldehyde may also be at greater risk of leukemia. It has been demonstrated that benzene can cause gene duplicating mutations in human bone marrow. Gene translocation in peripheral blood cells, and chromosome-specific aneuploidy can also be linked to leukemia (Smith 1996). Studies of 26000 industrial workers who were exposed to formaldehyde concluded that formaldehyde may cause leukemia in humans (Hauptmann, Lubin et al. 2003).

Another cause of leukemia is chemotherapy that uses alkylating agents. Children who were treated for cancer using alkylating agents have a 4% higher chance to develop leukemia twenty years after cancer treatment than the ones who went through radiation therapy (Tucker, Meadows et al. 1987).

Down's syndrome and some other genetic diseases caused by abnormal chromosomes can also increase the risk of leukemia. Patients with Down's syndrome have a 10-20 fold higher risk of developing leukemia compared to the general population (Fong and Brodeur 1987). Most people who have these risk factors do not develop leukemia and many people who develop leukemia have none of the risk factors.

The Philadelphia chromosome

About 90% of CML patients have a gene mutation called the Philadelphia chromosome (John 2003; Kurzrock, Kantarjian et al. 2003). The Philadelphia chromosome results from translocation of the *Abelson* gene from chromosome 9 to the breakpoint cluster region (*Bcr*) on chromosome 22 (John 2003) (Figure 1a, Page 5). The position where translocation occurs within the *Bcr* gene varies, therefore a number of different size proteins are translated from RNA transcripts produced from different translocated chromosomes. Therefore, the Bcr-Abl proteins are sized at 190, 210, and 230 kDa (Kurzrock, Kantarjian et al. 2003). The

Philadelphia chromosome is a somatic rearrangement and is therefore not passed from parent to child.

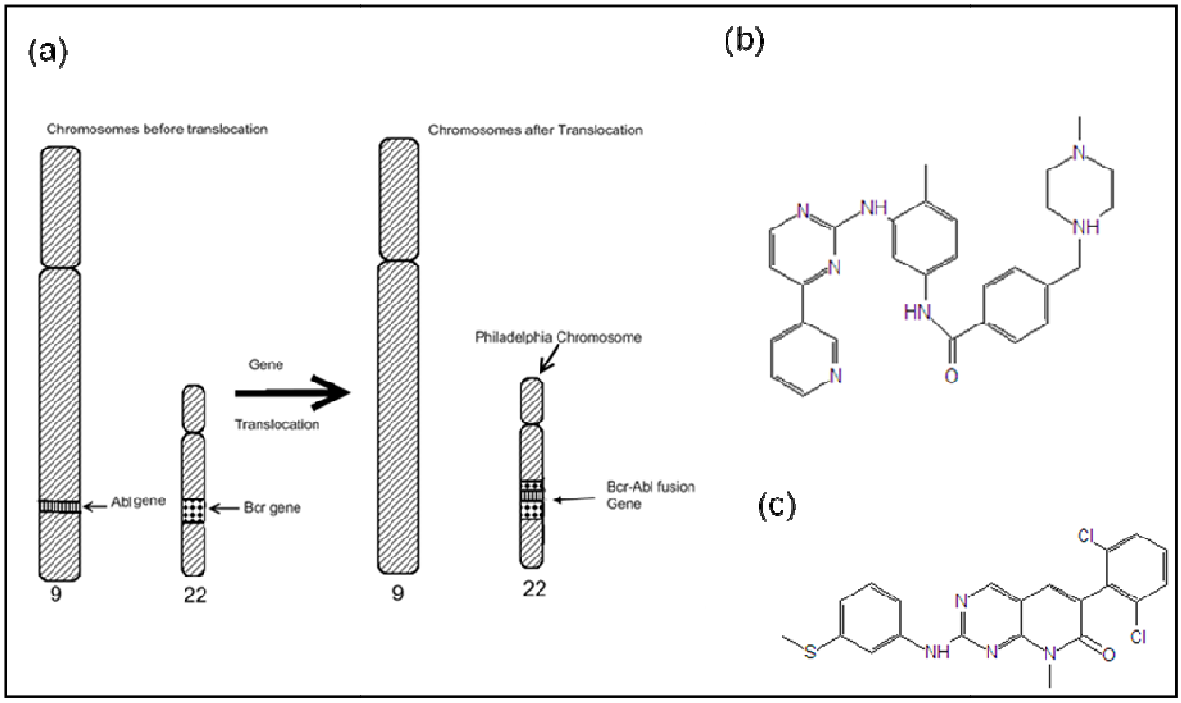

Figure 1: The Philadelphia Chromosome, Gleevec, and PD173955. Shown is (a) the translocation of the *Abl* gene from chromosome 9 to the *Bcr* gene on chromosome 22. The fused chromosome is called Philadelphia Chromosome, (b) the structure of Gleevec, and (c) the structure of PD173955.

Studies done by one group reported that the Bcr-Abl RNA transcript is found in healthy individuals at low levels. This group found the Bcr-Abl RNA in the blood in 23 out of 73 healthy adults, and in the blood of 1 out of 22 children (Biernaux, Loos et al. 1995). Even though the presence of the *Bcr-Abl* gene or transcript is associated with leukemia, it is very possible that this particular translocation is not

sufficient to initiate the disease. In later stages of leukemia it has been shown that mutations within this translocation are the reason for the multi drug resistance (MDR).

Abl protein kinase

The Abl protein kinase expressed by humans is 145 kDa (Kurzrock, Kantarjian et al. 2003). The N-terminal half of Abl (60 KDa) is homologous to the Src family of tyrosine kinases (Van Etten 1999; Nagar, Hantschel et al. 2003). It contains SH2 and SH3 domains and the tyrosine kinase domain. The SH2 and SH3 domains mediate protein-protein interactions and are involved in signal transduction. The Abl protein kinase is a nonreceptor tyrosine kinase. Several functional domains have been identified in Abl. The C-terminal domain includes a nuclear localization signal, DNA binding domain, and actin binding domain. Normal Abl phosphorylation is tightly regulated by the N-terminus through auto-inhibition and loss of this region through fusion creates unregulated kinase activity. The mechanism of regulation is not fully understood (Nagar, Hantschel et al. 2003).

Bcr protein kinase and Bcr-Abl fusion protein kinase

The *Bcr* gene is located on the long arm of chromosome 22, and is translated into two major proteins that have molecular weights of 130 kDa and 160 kDa. They are located in both the nucleus and cytoplasm. Like c-Abl the Bcr protein has

multiple domains that are involved in multiple functions. Two domains on the C-terminal half of Bcr are involved in two major signaling pathways in eukaryotes (phosphorylation and guanosine triphosphate binding) (Kurzrock, Kantarjian et al. 2003). The two domains that are involved in activation of c-Abl have been identified. Domain 1, which consists of the amino acids 1-63, is responsible for activating the tyrosine kinase activity. The amino acids 176-242 are capable of binding to the SH2 domain of Abl *in vitro* (McWhirter, Galasso et al. 1993).

Depending on the location of the *Bcr* gene fusion, two fusion proteins are translated with very similar activities: $p210^{Bcr\text{-}Abl}$ and $p190^{Bcr\text{-}Abl}$ (Kurzrock, Kantarjian et al. 2003). The $p190^{Bcr\text{-}Abl}$ variant has higher tyrosine kinase activity and is associated with the more aggressive form of the disease (Lugo, Pendergast et al. 1990).

Both forms of the Bcr-Abl protein kinases interact with activators of the Ras signaling pathway through binding to the SH2 domains of Grb2, Scr, and Shc. They also interact with intracellular substrates to cause cytoskeletal structural deformity. In addition, they interact with modulating proteins such as Bcl-2 or Bad, that are involved in suppression of cell death and apoptosis. Expression of the Bcr-Abl fusion proteins affect the DNA damage response process that is involved in DNA repair (Kurzrock, Kantarjian et al. 2003).

In summary the *Bcr-Abl* fusion gene produces a deregulated Bcr-Abl tyrosine kinase, which is the molecular basis of CML. Bcr-Abl is capable of auto-phosphorylating itself, inducing cells to proliferate and causing cancerous cells to

suppress apoptosis, which causes a large number of stems cells to develop into granulocytes and blast cells.

CURRENT TREATMENT

Tyrosine Kinase Inhibitor (Gleevec)

In 2001, the FDA approved a new revolutionary drug, a tyrosine kinase inhibitor called Imatinib mesylate or “Gleevec” (also known as STI571 and CGP57148B) (Figure 1b, Page 5) (Kurzrock, Kantarjian et al. 2003). Early results showed high efficacy of Gleevec and low toxicity which made Gleevec very attractive for treatment of CML patients. Gleevec is used to treat CML patients in all three phases, and is also prescribed for patients who have gastrointestinal kit-derived stromal tumors. It is a member of the 2-phenylaminopyrimidine class of compounds that was developed by Ciba-Geigy (now Novartis Pharmaceuticals) (Nagar, Bornmann et al. 2002; Goldman 2004). In addition to inhibition of the Abl tyrosine kinase, this drug potently inhibits other tyrosine protein kinases: the Kit (receptor for stem cell factor), the platelet-derived growth factor receptor (PDFGR-A and B), the *Abelson* related gene (ARG), and possibly other unidentified kinases (Goldman 2004).

The fusion of *Bcr* to *Abl* causes the Bcr-Abl tyrosine kinase to be almost always in the active conformation, but the tyrosine kinase dynamically cycles between inactive and active conformations. Crystallographic studies have shown

that Gleevec binds to the ATP binding site on the unphosphorylated, inactive conformation of the Abl kinase (Nagar, Bornmann et al. 2002). This suggests that binding of Gleevec might lock Bcr-Abl tyrosine kinase in its inactive form. Another mode of Gleevec inhibition is to bind newly synthesized Bcr-Abl tyrosine kinase. Initial treatment of CML patients with Gleevec showed extraordinary results, because it destroyed 90 percent of cancerous cells in the chronic phase.

Problems with Gleevec

Increased resistance to Gleevec and therapy failures are observed in patients with advanced CML. Because Gleevec is only effective against the inactive Bcr-Abl tyrosine kinase, it has been shown that it is much less efficient in patients who are in the blast crisis phase of CML (Druker, Sawyers et al. 2001).

Studies using Bcr/Abl$^+$ cell lines resistant to Gleevec showed that acquired resistance can be associated with increased expression of the Bcr-Abl protein, which is usually due to gene amplification (le Coutre, Tassi et al. 2000; Weisberg and Griffin 2000; Gorre, Mohammed et al. 2001). There are also cases where resistance to Gleevec occurred in cell lines or patients who were not previously exposed to Gleevec. When human leukocytic cells (LAMA84) were incubated with increasing concentrations of Gleevec for six months, they showed a 10 fold higher IC50 for Gleevec, increased concentration of Bcr-Abl, and higher Bcr-Abl mRNA levels than parental sensitive cell lines,. These more resistant cell lines showed 14 copies of

the fused *Bcr-Abl* gene per cell compared to the 4 copies that were present in the parent cells.

Because Gleevec binds to the ATP binding site on the Abl kinase domain, acquired resistance to Gleevec led researchers to look for possible mutations in the ATP binding pocket that prevented binding of Gleevec, while permitting binding of ATP. One group reported mutations in 17 different residues in the kinase domain (Branford, Rudzki et al. 2003). Another group discovered that a single amino acid substitution in a threonine residue of the Abl kinase domain, known to form a critical hydrogen bond with the drug, is sufficient to prevent Gleevec binding to the kinase domain (Gorre, Mohammed et al. 2001).

The biological availability of Gleevec is reduced by the over expressed alpha-1 acid glycoprotein (AGP) in CML cancer cell lines. AGP binds Gleevec and blocks its diffusion from the blood to cancerous cells (Gambacorti-Passerini, Barni et al. 2000; Hamada, Miyano et al. 2003).

Other types of treatments

Desatinib, also known as BMS-354825**,** is another tyrosine kinase inhibitor that is prescribed to patients who are in the later stages of the CML (Talpaz, Shah et al. 2006). This drug is only prescribed to patients who did not respond to Gleevec or can not use it for another reason. Currently this drug is being tested to be used to

treat patients in the initial stages of CML, to improve treatment of CML patients by avoiding problems associated with Gleevec resistant CML patients.

Chemotherapeutic drugs are used to treat CML patients by either killing the cancer cells or stopping them from dividing. They can be taken by mouth, injected into veins, or injected into the organ that needs to be treated. The pathway by which the drug is delivered to the CML patient depends on the stage of CML. Damage to healthy cells is commonly observed with the use of chemotherapeutic drugs, which lowers the patients' immune system, increases bleeding and a loss of energy. Some chemotherapy drugs may affect cancer patients' fertility. Women's menstrual cycles may occur irregularly and stop and men may stop producing sperm. Some of these side effects become permanent.

Biological therapy is a treatment that uses the patient's immune system to fight cancerous cells. Interferons are proteins that are produced by the body to fight foreign cells. They can be give intravenously, intramuscularly, or subcutaneously to patients. Flu-like symptoms are observed with each interferon administration. Depression and suicide have been reported with patients who use interferons.

Another way to treat patients with CML is with a combination of high dose chemotherapy and stem cell transplantation. In this treatment regiment high doses of chemotherapeutic drugs are given to the patients and their damaged blood cells are replaced with immature donor blood cells.

Donor lymphocyte infusion is a treatment in which donor lymphocytes are injected through one or multiple infusions into the patients. Infused lymphocytes recognize the patient's cancer cells as foreign then attack and kill them. Donor lymphocyte treatment has all the side effects associated with chemotherapy and radiation.

The last option available to CML patients is splenectomy where the patient's spleen is surgically removed. This treatment is performed after all the above treatments are unsuccessful. Splenectomy is more effective in patients who have CLL, and has little effect with patients who are diagnosed with CML. Studies with patients who went through splenectomy in early CML show no increase in survival rate. Splenectomy may benefit CML patients in more advanced phases of leukemia, and patients who underwent bone marrow transplantation (Mesa, Elliott et al. 2000).

PROPOSED TREATMENT

Due to the resistance problems that occur in patients who are treated with Gleevec, combined with the dangerous side effects associated with other treatments, it is necessary to develop an effective method to treat CML. From the search for a more effective drug, a new class of compounds emerged as a possible solution to problems associated with current treatments. The pyrido[2,3-d]pyrimidines constitute a large group of compounds that were developed to target different tyrosine kinases. These compounds were initially developed as broadly

active inhibitors of several tyrosine kinase such as Src, platelet-derived growth factor receptor and fibroblast growth factor receptor (FGFR) (Wissing, Godl et al. 2004). PD173955 is a pyrido[2,3-d]pyrimidine that was shown to potently inhibit the Bcr-Abl and c-kit tyrosine kinases *in vivo* (Wisniewski, Lambek et al. 2002; Wissing, Godl et al. 2004) (Figure 1c, Page 5). PD173955 is capable of inhibiting the kinase activity of Bcr-Abl with an IC50 of 1-2 nM *in vitro*. Crystallographic studies show that PD173955 can recognize multiple Bcr-Abl kinase conformations, which could explain its higher efficacy as an inhibitor (Nagar, Bornmann et al. 2002). PD173955 binds Bcr-Abl tyrosine kinase in its active and inactive conformations and is very efficient against most Gleevec resistant CML cell lines.

PD173955 also binds other kinases, such as p38, GAK, and RICK (Wissing, Godl et al. 2004) but with lower affinity compared to Src and Abl kinases. Other kinases such as Mek1, Jnk2, and Aurora A required 1,000-10,000 higher concentration of PD173955 derivative to achieve half of the maximum inhibition. The same group reported the IC50 for Abl and Scr kinases in the subnanomolar range by PD173955 derivative, which is about 30 fold less then previously reported by others. They suggest that possible reason for the discrepancy is the amount of enzyme used in their assays compared to others.

PD173955 has a significant antiproliferative activity due to a potent arrest of mitotic progression through inhibition of the Src family of tyrosine kinases (Moasser, Srethapakdi et al. 1999). This effect was observed in cancer cell lines of all types including breast cancer cell lines, prostate cancer, ovarian cancer, colon cancer,

lung cancer, epidermal cancer, as well as non-transformed cell lines: MCF-10A and NIH-3T3. In MDA-MB-468 breast cell lines PD173955 inhibits Src and Yes kinase activities (Moasser, Srethapakdi et al. 1999).

A major concern for the pyrido[2,3-d]pyrimidines is their broad specificity for other protein kinases (Wissing, Godl et al. 2004). But the broad specificity of compounds such as PD173955 can be used to attack leukemic cells at different cellular targets by inhibition of several tyrosine kinases involved in the cell proliferation. In addition, there are data from medicinal chemistry studies showing that the specificity of pyrido[2,3-d]pyrimidine based compounds can be efficiently improved (Wissing, Godl et al. 2004). For example, by replacing the 6-(2,6-dichlorophenyl) moiety with a 6-(3',5'-dimethoxyphenyl) produced a highly selective FGFR tyrosine kinase inhibitor (Hamby, Connolly et al. 1997).

There is not much known of the pharmacokinetic properties of the pyrido[2,3-d]pyrimidines. This is mostly due to their limited solubility, and the inconsistent dose-dependent responses observed in mouse xenografts (Wissing, Godl et al. 2004). The limited solubility is the major problem associated with the pyrido[2,3-d]pyrimidines and therefore not too much research has been performed to improve their specificity. The limited solubility of PD173955 in aqueous environments was confirmed by a researcher in our lab (Marjan Mokhtarian). The maximum solubility of PD173955N in 5% DMSO was 35 µM. Although PD173955 is potent inhibitor of Bcr-Abl, its limited solubility in water makes it undesirable as a drug. This is a reason, why the benefits of these compounds are not explored further. Use of

compounds like PD173955N in binding assays *in vitro* is very challenging task, because it is very difficult to reach high enough concentrations necessary for these assays.

The use of aptamer technology may improve efficiency of pyrido[2,3-d]pyrimidines

Improved PD173955 solubility and targeting can be addressed by the use of carrier molecules that decrease exposure of the hydrophobic molecules to the aqueous environment and target the appropriate receptors. Nucleic acid aptamers provide a means for developing drug carriers. Aptamers are single stranded RNA or DNA sequences that bind their targets with high specificity and affinity (picomoles to micromoles). Since their first introduction in the 1990s there have been a few hundred aptamers selected to various targets. These targets include small molecules, amino acids, peptides, and proteins (Proske, Blank et al. 2005). Most aptamers are obtained using a technique called SELEX “Systematic Evolution of Ligands by EXponential enrichment”. Using this method it is possible to select rare nucleic acids with the desired characteristics from a very large number of nucleic acid sequences. The technique was developed by two groups in 1990. One group selected an aptamer that recognizes the T4 bacteriophage DNA Polymerase (Tuerk and Gold 1990), and the other group selected an aptamer that binds organic dyes (Ellington and Szostak 1990).

Aptamers are generally 15-40 nucleotides long and can be composed of a chemically modified backbone (2'-fluoro or 2'-O-methyl), which increases their half-lives *in vivo* from hours to days. They can be chemically synthesized using standard nucleic acid synthesis methods, which makes them attractive therapeutic agents. Aptamers are selected from a pool of nucleic acids (10^{12}-10^{15} molecules), containing oligonucleotides each with a different sequence. These oligonucleotides within the pool provide a number of three-dimensional conformations from which to select aptamers, making them ideal tools to select rare well-defined conformations to bind their targets tightly.

Aptamer functions *in vivo*

Aptamers selected *in vitro* have very similar functions when tested *in vivo*. For example, when an RNA aptamer to the nucleocapsid protein of the human immunodeficiency virus-1 was expressed in cells as a intracellular RNA aptamer "intramer", it inhibited packaging of the viral genomic RNA (Kim and Jeong 2004). The same aptamer completely abolished nucleocapsid binding to the stable transactivation response hairpin and psi RNA stem-loops of HIV-1 RNA (Kim and Jeong 2004).

Another aptamer, that was shown to be functional inside a multicellular organism, is a anti B52 protein aptamer (Shi, Hoffman et al. 1999). B52 is a member of the *Drosophila* SR protein family, which is responsible for mRNA splicing.

Previous work showed that B52 is essential for Drosophila life. Deletion and over-expression of B52 results in death or causes critical morphological deformation of the organism (Ring and Lis 1994). Shi *et al.* (Shi, Hoffman et al. 1999) generated a *Drosophila* that both over-expressed B52 and expressed an aptamer that recognized B52. They used the generated *Drosophila* to demonstrate efficacy of the aptamer *in vivo.* Reversal of the morphological deformation that was associated with B52 expression was observed due to anti-B52 suppression by the aptamer.

PDGF-B is involved in the regulation of interstitial fluid pressure (IFP). Elevated IFP is a property of solid tumors (an abnormal mass of tissue that does not contain fluid or cysts) that prevents delivery of chemotherapeutic drugs. The IFP can be also associated with increased tumor size, malignancy and poor prognosis in cancer patients. Blocking PDGF-B in KAT-4 thyroid carcinoma tumors with the tyrosine kinase inhibitor Gleevec dramatically decreased the tumor IFP *in vivo* and increased uptake of the chemotherapeutic drug Taxol.

The ability to chemically stabilize aptamers against nuclease degradation through 2'-O-methyl modification of the purine nucleotides, and attaching them to higher molecular weight polyethylene glycol (PEG) makes them good tools for extracellular drug delivery. One group selected an aptamer that blocks PDGF-B binding to its receptor with a dissociation constant in the nanomolar range (Kd ~100 nM) and attached it to PEG (Green, Jellinek et al. 1996). Treatment of KAT-4 xenograft mice with the PEG-conjugated PDGF-B aptamer decreased IFP *in vivo*

and increased uptake of Taxol (Pietras, Rubin et al. 2002). Here we can see the advantage of using an aptamer over a tyrosine kinase inhibitor like Gleevec.

Aptamers are newly developed reagents and their utilization in the clinical applications is so far very limited. But one aptamer is already approved for clinical use and a number of other aptamers are in the process of development for medical use. They are being developed for topical and intravenous applications in the clinic. The first FDA-approved aptamer is the polyethylene glycol linked anti-VEGF aptamer, NX1838 also known as Macugen, which is used to cure AMG “age related macular degeneration” and diabetic retinopathy (Pendergrast, Marsh et al. 2005; Ng, Shima et al. 2006). Vascular endothelial growth factor (VEGF) is responsible for blood vessel leakage and their advanced expansion towards the retina of the eye. The abnormal vessels leak fluid, blood, and lipids, which damage the photoreceptors of the eye. If left untreated 45 percent of these unhealthy eyes will develop moderate vision loss and 22 percent will develop severe vision loss. Macugen blocks VEGF’s actions, which prevents the symptoms associated with VEGF’s actions from occurring. With a single ocular injection of Macugen, 80 percent of AMD patients had improved or stabilized vision after three months. All patients who continued to receive the ocular injections showed improved vision compared to the patients who didn’t receive the injections (Pendergrast, Marsh et al. 2005).

Another aptamer that is under development for medical use is a thrombin inhibitor, a drug called ARC183. It is being developed by Archemix for potential use as an anticoagulant in coronary artery bypass graft (CABG) surgery. The only FDA

approved drug to currently serve as an anticoagulant is heparin. The advantages of heparin include a low cost of synthesis, and the fast reversal of the heparin side effects by protamine. The serious side effects associated with the use of heparin/protamine include bleeding and platelet count reduction. There is a strong need for a new low cost drug. ARC183 is a strong anticoagulant *in vitro*, and inhibits thrombin-catalyzed activation of fibrinogen, and thrombin-induced platelet aggregation in cynomolgus Macaques (*Macaca fascicularis)* (Griffin, Tidmarsh et al. 1993).

An example where an aptamer can be used to suppress mesangial cell proliferation is a PDGF-B (ARC127) binding aptamer in rats. Certain residues of ARC127 aptamer have been modified with 2-O-methyl moieties to increase its stability *in vivo* without loss of aptamer affinity. ARC127 is being considered for medical applications where PDGF-B has been implicated. The target diseases include: glomerulonephritis, pulmonary hypertension, and intimal hyperplasia following percutaneous transluminal angioplasty (Floege, Ostendorf et al. 1999; Vaish, Larralde et al. 2003).

In the past two decades multiple nanoparticle carriers have been developed to deliver highly hydrophobic drugs to their targets (Liangfang Zhang 2007). Liposomes and cationic core shell nanoparticles have been used to deliver drugs and DNA plasmids to cells. The surface of the nanoparticles can be coated with aptamers so they would deliver drugs to specific targets. One research group developed a system where they were able to deliver hydrophobic and hydrophilic

chemotherapeutic drugs to prostate cancer cells intracellularly using aptamer coated nanoparticles (Liangfang Zhang 2007). Prostate specific membrane antigen (PSMA) is expressed on the surface of prostate cancer cells. This group used an aptamer that binds PSMA and attached it to a nanoparticle to deliver chemotherapeutic drugs. The aptamer was preloaded with the intercalating hydrophilic drug and the nanoparticle also contained the hydrophobic chemotherapeutic drug. The uptake of chemotherapeutic drugs by prostate adenocarcinoma cells was modeled using the hydrophobic and the hydrophilic dyes and was visualized with cells that express PSMA using fluorescence microscopy. They reported no drug uptake by cancer cells that do not express PSMA compared to cells that express PSMA. This is an example of targeted drug delivery that can be achieved with aptamers.

All examples discussed here show how aptamer technology has advanced since aptamer introduction in 1990. Aptamers can be used for a number of different applications. The aptamers' properties and functions are compared to monoclonal antibodies, but they differ from antibodies in many ways. Unlike for antibodies, the production of aptamers can be done *in vitro* without the use of animals or cell lines, and aptamers can be selected to almost any target including toxic ones. Aptamers are chemically produced, allowing the attachment of a number of different reporter molecules or other molecules in precise locations on the aptamer (Davis, Lin et al. 1998). They are stable under a wide range of buffer conditions, and can be denatured and renatured without any loss of affinity, making them easily stored. The whole SELEX process required to select an aptamer can be done in 6-8 weeks.

Unlike for antibodies, the aptamers can be reselected to increase their affinity or further modified to change their specificity. When compared to the antibody the design and production of aptamers is very inexpensive. These are the characteristics that make aptamers more attractive then antibodies.

The SELEX process is very simple and can be done on the bench top or by automated systems in a short period of time (Cox, Hayhurst et al. 2002; Eulberg, Buchner et al. 2005). The basic procedure involves a number of iterative rounds that consist of binding, partitioning, and amplifying the desired nucleic acid from a combinatorial pool that consists of up to 10^{16} different sequences. Even though the basic procedure is very simple, even small alterations can produce unwanted results (Murphy, Fuller et al. 2003). One has a number of different decisions to make before performing SELEX. Some of the decisions which seem to be most critical for successful SELEX include the initial binding conditions, the separation method, and the elution method. The first selection processes were performed by attaching the target to a solid support and passing the selection pool through it (Tuerk and Gold 1990). Depending on the size of the target more recent selection procedures do not use target attached to the solid support, but perform the binding reaction step in solution. The target nucleic acid complex can be captured by the use of a solid support like the agarose beads or by nitrocellulose membranes if the target is large enough. For smaller targets attachment to a solid support is unavoidable at this time. Dissociation of the bound nucleic acids from the target can be done by passing a high concentration of target through the column or the filter. If the target

molecule is scarce or insoluble at high concentrations, denaturing reagents such as concentrated urea can be use to elute the aptamer pool from the target. These methods consume target concentrations in the range of 1-100 mM and oligonucleotides pools concentrations in the range of 0.001 to 1 mM. Once the desired characteristics of the selected aptamer population are achieved, the constituents of the remaining population are cloned and the cloned oligonucleotides sequenced. After the aptamer candidate with the lowest dissociation constant is chosen, the size of the aptamer is reduced to a minimum binding region. Usually optimization leads to increased binding affinity and specificity of the aptamer due to a decrease in a number of competing and nonbinding conformations (Pendergrast, Marsh et al. 2005).

SELEX is best applied when used to generate aptamers against large molecules, because they offer larger surface areas for the aptamer target interaction (Hamula, Guthrie et al. 2006). Target molecules must be stable, and easily captured. Proteins make ideal aptamer targets and that is why there are so many aptamers generated against them. The SELEX procedure to small molecules has not been as successful as to larger molecules (Hamula, Guthrie et al. 2006). This is mostly due to the small surface area that the nucleic acids can bind. Aptamers generated against small molecules have K_Ds in that range from low μM to mM, compared to those of larger targets that are in picomolar to the mid nanomolar range.

For this study PD173955 was chosen as an aptamer target because of its great potential for inhibition of the Bcr-Abl tyrosine kinase. Also this compound was chosen due to its low solubility. PD173955 represents many potent compounds with low solubilities produced by the chemical companies. We intend to use aptamer technology to overcome the problems associated with PD173955. If successful, this approach could be applied and be used with other members of the pyrido[2,3-d]pyrimidines class of compounds and with other drugs.

Aptamers can be used as carriers to encapsulate hydrophobic compounds like PD173955 to protect them from aqueous environments in which they have low solubility. The problems associated with these types of compounds before they can be used for medial applications are low solubility resulting in low concentrations inside the cell. The advantage of using aptamers to solve this problem is because the complexity of the random oligonucleotides in the starting original pool can take numerous tertiary conformations and can bind to almost any target. Aptamers often completely wrap around their targets upon binding. This characteristic of an aptamer can be used to increase the concentration of the compounds inside of the cell. A novel and efficient model to help protect insoluble compounds like PD173955 from aqueous environments and to increase its concentration inside of the cancerous cells would be very beneficial. The first step is to select an aptamer that is capable of recognizing and binding PD173955. PD173955 has very limited solubility in aqueous environment. Even though the original pool contains a large number of different tertiary structures of oligonucleotides, selecting the one that can bind a

target with as low a solubility as PD173955 was a very challenging task. The affinity of the selected RNA for PD173955N is much lower than affinity of Bcr-Abl protein for PD173955.

In this thesis the data from SELEX experiments to select an aptamer that recognizes PD173955 will be presented. The size of the selected putative aptamer was minimized from 78 to 37 nucleotides long. The selected aptamer binds PD173955 with high affinity in intracellular buffer conditions and at a temperature of 37^{o}C. PD173955 is an ATP analog, but the selected aptamer has very low affinity for adenosine and ATP under the same conditions.

The selected aptamer binds at least one other insoluble compound that belongs in same class of compounds as PD173955. Based on the solubility of the compounds that were used and their structures, some conclusions can be made regarding the aptamer's specificity.

CHAPTER 2: SELECTION OF AN RNA APTAMER TO PD173955N THROUGH SELEX

INTRODUCTION

Using SELEX, an aptamer was selected that can bind PD173955 in water based buffers that approximate intracellular salt concentrations. The aptamer has a Kd of 1-3 μM for PD173955 and could be used to target the compound to specific cells. Although PD173955 is an ATP analog, the aptamer has low affinity for ATP and adenosine. However, the aptamer binds with relatively high affinity to another compound that is chemically related to PD173955. This suggests that the selected RNA aptamer to PD173955B (Figure 2a, Page 26) might be applied directly as a carrier for a range of pyrido[2,3-d]pyrimidines compound. Alternatively, aptamers can be further evolved by a procedure called “doping” to alter their specificity for related molecules.

The RNA SELEX was performed in the following way (Figure 3, Page 28). A single stranded randomized DNA pool was synthesized and it was PCR amplified or extended to generate the double stranded DNA pool. Using this DNA pool, RNA was generated by *in vitro* transcription and simultaneously radio-labeled for easier tracking. The radio-labeled RNA was mixed with the PD173955B. The RNA/target complexes were separated from non binding RNA molecules using a filter apparatus. Then the RNA was reverse transcribed and PCR amplified to generate

the dsDNA pool for the next round. After sufficient binding or no increase in binding from previous rounds was achieved, the PCR amplified dsDNA pool was cloned and sequenced. The sequences were aligned and families identified as putative aptamers. The affinities of the putative aptamers for PD173955N (Figure 2b, Page 26) were checked by isothermal titration calorimetry (ITC).

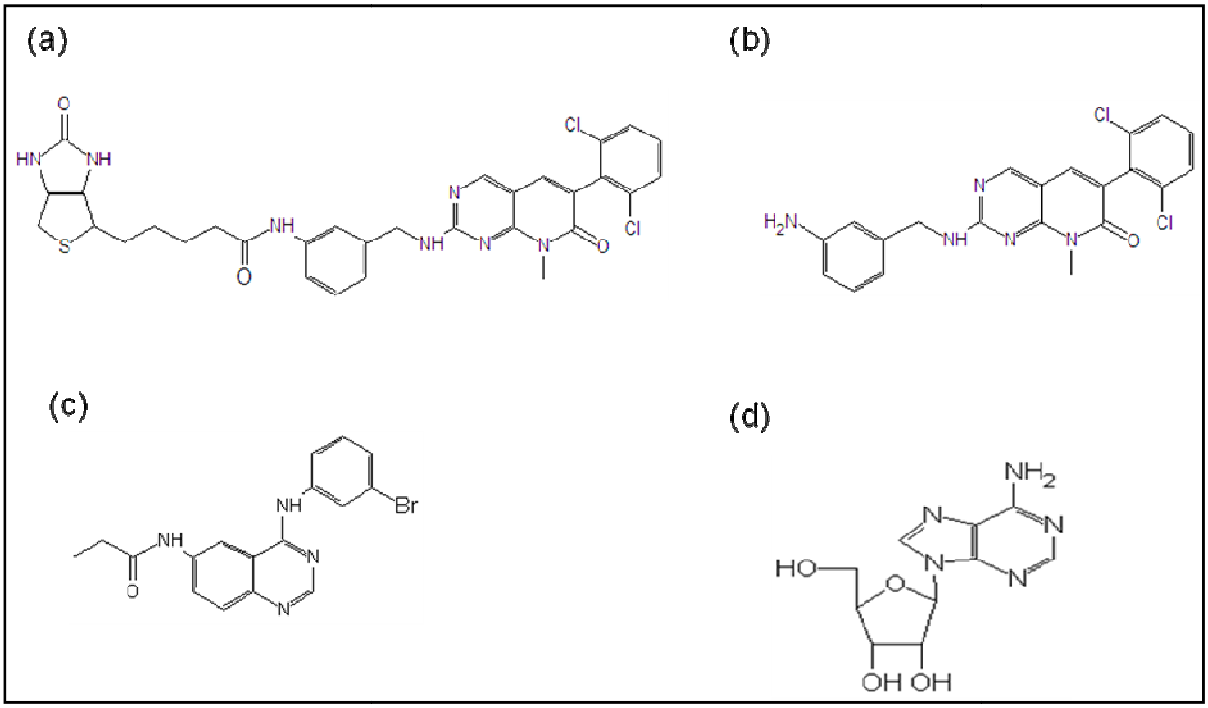

Figure 2: The structures of several pyrido[2,3-d]pyrimidines and adenosine. The Structures of (a) PD173955B, (b) PD173955N, (c) 4-[(3-Bromophenyl)amino]-6-propionylamidoquinazoline (PD174265), and (d) adenosine.

A number of different methods were tested to select RNA aptamers to PD173955. These trials were not successful. In the earlier selections a more

traditional method to select an aptamer was used. This method involved covalently attaching PD173955N to Sepharose 4B beads and making a small column that was used for the selection procedure. By using this method three problems appeared. First, nonspecific binding was high so more then 50% of the RNA molecules bound to the beads that didn't have any PD173955N attached. The second problem was that the beads had too many reactive groups for PD173955N attachment and the concentration of PD173955N was not easily controlled. Covalently attaching lower concentrations of the target to the Sepharose 4B beads was unsuccessful. The third possible reason why this selection was unsuccessful may have had been due to the complexity of the initial random pool. To prepare the initial dsDNA random pool only a small portion of the ssDNA pool was PCR amplified, which resulted in multiple copies of a subset of the molecules in the initial dsDNA pool. In the later successful selections DNA extension instead of PCR was used to generate the initial dsDNA pool. The advantage of using DNA extension over PCR amplification is that the complexity of the initial double stranded pool is retained. A disadvantage of that is the copy number of the each dsDNA molecule is lower.

Another unsuccessful attempt at SELEX involved selections of the RNA aptamers using Streptavidin beads that were pre-coated with the biotinylated PD173955B (Figure 2a, Page 26) derivative. After six rounds of selection no enrichment was observed and these selection experiments were stopped.

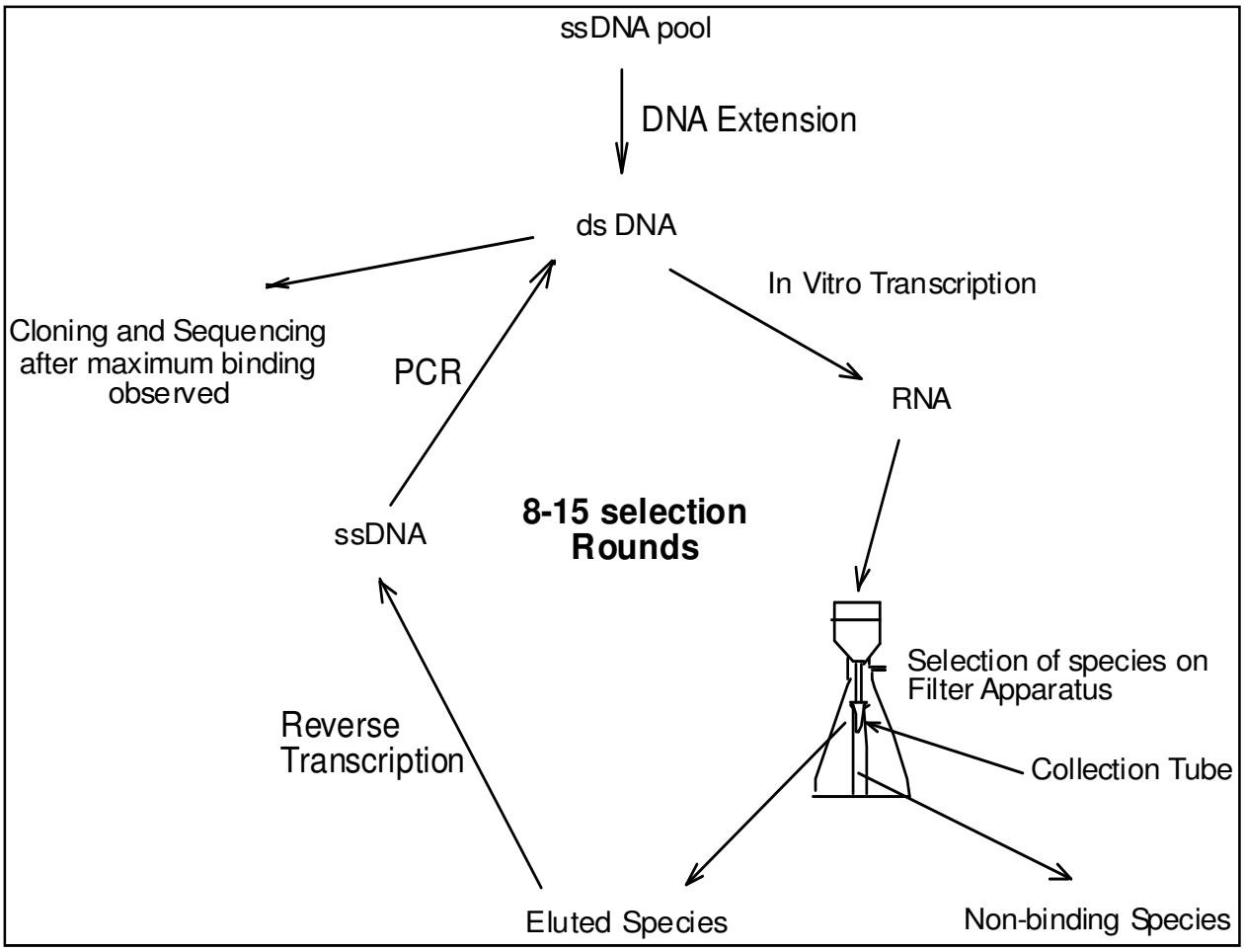

F**igure 3: RNA SELEX.** The basic procedure for RNA SELEX is shown.

MATERIALS AND METHODS

DNA library construction

The DNA oligonucleotide template library named Oligo 487: 5'-GCCTGTTGTGAGCCTCCTGTCGAA(53N)TTGAGCGTTTATTCTTGTCTCCC-3' with N symbolizing an equimolar mixture of A, C, G, and T, was synthesized (Integrated DNA Technologies, Coralville, IA). The oligonucleotide primers used in

reverse transcription and PCR experiments had the following sequences: Oligo 484: 5'-TAATACGACTCACTATAGGGAGACAAGAATAAACGCTCAA-3' and Oligo 485: 5'-GCCTGTTGTGAGCCTCCTGTCGAA-3′. All pH values cited in this thesis were measured at 23°C. For the first round of SELEX double-stranded DNA pools were generated in the following way. Twenty four 100 µl reactions containing 1.67 µM of Oligo 487, 0.5 mM dNTP, 3.33 µM oligo 484, and 0.03 U/µl DNA Taq Polymerase (GenScript) in 50 mM KCl, 10 mM Tris HCl (pH 8.55), 1.5 mM $MgCl_2$, 0.1% Triton X-100 were incubated at 95 ℃ for 10 min, at 65 ℃ for 30 min, and at 72 ℃ for 99 minutes using the Multi GENE II PCR minicycler. The generated dsDNA was ethanol precipitated by adding 2.5 volumes of 100% ethanol and 0.1 volume of 3 M NaOAc and incubated at -80 ℃ for 30 minutes. The sample was centrifuged for 15 minutes and the precipitated dsDNA was dissolved in 120 µl ddH_20 (distilled, deionized water). The dissolved dsDNA was resolved through a 12% PAGE in TBE (90 µM Tris-Borate, 2 µM EDTA, pH 8.5) to separate the primer and the ssDNA that was not extended. The top band was cut out, crushed, and eluted overnight at 37 ℃ in 300 mM NaOAc, 10 mM EDTA, pH 8. The eluted DNA was phenol/chloroform extracted and ethanol precipitated to remove polyacrylamide contaminants. The pellet was resuspended in 90 µl of ddH_20 and the dsDNA quantified by measuring absorbance at 260 nm. The 260/280 ratio was used to monitor the purity of dsDNA.

RNA synthesis and purification

RNA was prepared by *in vitro* transcription using the AmpliScribe™ T7-*Flash*™ Transcription Kit (Epicentre, Madison, WI). The transcription reaction was carried out at 37 ℃ for 4-6 hours. For the "body-labeled" RNA, 166 nM of α-P ^{32}-ATP in combination with 7.5 mM of each NTP (ATP, UTP, CTP, GTP) was included in the reaction mixture. Following DNase digestion (1 MBU per 20 µl), the RNA was ethanol precipitated by adding 2.5 volumes of 100% ethanol, and 0.1 volume of 3 M NaOAc and incubated at -80℃ for 30 minutes. The sample was centrifuged for 15 minutes and the precipitated RNA was dissolved in 8 M urea. The dissolved RNA was resolved through a 10% denaturing PAGE gel containing 7 M Urea in TBE at 200-300 volts. The band was visualized under a UV lamp, excised, gel crushed, and eluted overnight at 37 ℃ in 300 mM NaOAc, 10 mM EDTA, pH 8. The gel slices were centrifuged at top speed (Eppendorf, model 5415D), the supernatant containing the RNA was removed and the RNA ethanol precipitated. The RNA was resuspended in DEPC H_2O (0.01% diethyl pyrocarbonate in dH_20, autoclaved at 120^{o}C for 1 hour) and quantified by measuring the absorbance at 260 nm. The 260/280 ratio was used to check the purity of the RNA.

Determination of the molar extinction coefficients of the PD173955 derivative

Amino labeled and biotin labeled derivatives of PD173955 were synthesized by Dr. George Kraus' lab (ISU, Ames, IA) (referred as PD173955N and

PD173955B), dissolved in 100% DMSO and stored in -20^{o}C until use. PD174265 was purchased from Calbiochem (San Diego, CA), and stored in 100% DMSO at -20^{o}C (Figure 2c, Page 26). Adenosine was from Sigma (St. Louis, MO), and ATP was from Epicentre (Madison, WI). The structures of the compounds were drawn using WinDrawChem available at http://xdrawchem.sourceforge.net/windrawchem/.

The molar extinction coefficient (ε) for PD173955N was determined by UV absorbance based on Beer's Law ($A=\varepsilon cl$), where c stands for the molar concentration and l stands for the path length, which was 1 cm. A known mass of PD173955N was dissolved in 50% ethanol and 50% DMSO. The solution containing PD173955N was scanned from 200 to 800 nm using UV Spectrophotometer (Biowave, model S2100, WPA, Cambridge, England). The UV absorbencies were read of increasing concentrations of PD173955N. The absorbance readings vs. the concentrations of PD173955N were plotted using Microsoft Excel and ε was calculated.

Mathematical simulation of SELEX

Mathematical simulation of SELEX was used to set the optimal initial concentrations of the RNA pool and PD173955B (Levine and Nilsen-Hamilton 2007). The simulation model predicts the least number of selection rounds necessary to reach 100% of possible binding species based on the user input. For the simulation to work, the user needs to know the K_D of the initial RNA aptamer

pool, the approximate K_D of the best binding RNA aptamers within the pool, and the background binding of the initial pool.

To use the model the initial pool was grouped into 15 binding groups of aptamers with Group one having highest affinity for the target and the Group 15 the lowest. The advantage of using the model is that the user can set the selection pressure on the SELEX by changing the percentage of the target reduction with each additional round and see the simulated results. If the percent of the target reduction is set too high, no selection is observed, or it may take many extra rounds for the binding species from Group one to reach maximum percent bound. Also, if the background (everything else except target) is set too high, one may never obtain the maximum amount of the binding species.

A computational analysis was used to predict initial conditions, which required the insertion of estimates of the dissociation constant of the initial pool and of the aptamers to be selected. The affinity of the original pool for PD173955N and the percentage of the background binding were determined experimentally. Because PD173955 is an ATP analog, the best K_D of the aptamer to be selected was predicted to equal 1 µM, which is in the same range as for the ATP RNA aptamer (5-8 µM) (Sassanfar and Szostak 1993; Sazani, Larralde et al. 2004).

In vitro selection

SELEX was principally performed as described by Tuerk and Gold (Tuerk and Gold 1990). Briefly, “body” radio-labeled RNA was dissolved in selection buffer (300 mM KCl, 5 mM $MgCl_2$, 20 mM HEPES, 5% DMSO, pH 7.5).

Approximately 8000-16000 ultralink immobilized streptavidin beads (Pierce, Rockford, IL) were washed with 1 ml of selection buffer, by resuspending the beads in the selection buffer and spinning them down 2-3 times and discarding the supernatant. In the first selection round 0.5 nmoles of the S.R0 RNA pool in selection buffer was mixed with 1 nmole of PD173955B at 23 ℃ in 1 ml reaction.

The binding reaction was performed by slowly agitating the mixture by rotation at 23 ℃ for 30 minutes. Afterward, 16,000 prewashed immobilized streptavidin beads were added to the binding reaction and the reaction was incubated for an additional 30 minutes to capture the RNA/PD173955B complex. The mixture was filtered though a 0.44 µm filter on filter apparatus and washed 1 time with 1 ml of the selection buffer. The bound species were eluted with 8M urea at 95 ^{o}C and 1 ml fractions collected. The elutions were pooled, ethanol precipitated as described above, and dissolved in 20 µl of DEPC dd$H_2$0. Due to the low concentrations of RNA in the collected elutions, linear polyacrylamide (Sigma, St. Louis, MO) was used as carrier to help better precipitate the RNA. The precipitated RNA was reverse transcribed using SuperScript^{TM} III RNase H^{-} and reverse primer Oligo 485, (Invitrogen, Carlsbad, CA) in 50 mM Tris-HCl 75 mM KCl, 3 mM $MgCl_2$, 5 mM DTT (pH 8.3), at 50^{o}C for 1 hour and the reaction was stopped by incubating at 70^{o}C for 15 minutes. One half of the reverse transcription reaction was PCR amplified in 100 µl PCR reaction (50 mM KCl, 10 mM Tris HCl, 7.5 mM $MgCl_2$, 0.1% Triton X-100 Buffer, 2 µM primers, 1 mM dNTP, 0.5 U/µl Taq DNA Polymerase (pH 9.0) for 12-14 cycles, 3 minutes at 93^{o}C, 30 seconds at 93^{o}C, 1 minute at 65^{o}C, 1 min at 72^{o}C, and 5 minutes at 72^{o}C. The other half the reverse transcription

reaction was saved in case the PCR didn't work or the *in vitro* transcription was unsuccessful. To help increase mutations in the pool, 7.5 mM $MgCl_2$ and 1 mM dNTP were used in the PCR reactions. After each PCR amplification, the PCR product was resolved on 2% agarose in TAE buffer (40 µM Tris Acetate, 1 µM EDTA, pH 8) to verify the size of the amplicon. For negative selections, RNA pools were incubated with the streptavidin beads for 30 minutes to remove RNA species that bind specifically to the beads and the filter. The beads were washed once with 1 ml of selection buffer, and the flow-through and wash fractions were pooled and ethanol precipitated and the RNA was dissolved in the selection buffer. The dissolved RNA was mixed with PD173955B in the selection buffer and the next selection round was performed as above. Two SELEX experiments, named S569 and S570 were performed in parallel. After the first round in each SELEX experiment, the concentration of PD173955B was reduced either by 0 or 10% in each additional round. After the 12^{th} round of S570 and the 8^{th} round of S569, the ssDNAs were PCR amplified as described previously, and cloned into pcDNA 3.1 using the Directional TOPO expression plasmid kit (Invitrogen, Carlsbad, CA). The plasmids were chemically transformed into One Shot bacterial cells (Invitrogen, Carlsbad, CA), and the bacteria were grown in SOC media (2% Tryptone, 0.5% yeast extract, 10 mM NaCl, 2.5 mM KCl, 10 mM $MgCl_2$, 10 mM $MgSO_4$, 20 mM glucose) for one hour with shaking (250 rpm). The transformation mix was plated on LB (15g/l Bacto Agar, 10 g/l Bacto Tryptone, 5 g/l yeast extract, 10 g/l NaCl) culture plates with ampicillin resistance (50 µg/ml) and grown overnight in 10 ml of LB at 37^oC. Individual clones were picked and grown overnight in 10 ml of LB (50 µg/ml

ampicillin) at 37°C with shaking (250 rpm). Plasmids were extracted from 3 ml of each bacterial culture using the QIAprep Spin Miniprep Kit (Qiagen, Valencia, CA), and the plasmids sent for DNA sequencing (ISU DNA facility, Ames, IA). Sequences of the inserts within the sequences were found using Biology WorkBench, and aligned using BioEdit software (obtained at: //workbench.sdsc.edu/ and www.mbio.ncsu.edu/BioEdit/bioedit.html). The nomenclature given the clones obtained from the SELEX experiments is as follows. S###R##C##, where the first number is that assigned to the SELEX experiment, R## is round number, and C## is the clone number.

Measurement of binding affinities of the putative aptamers

The affinities of the selected aptamers to PD173955B were measured in solution by isothermal titration calorimetry (ITC) on a VP-ITC instrument (MicroCal, Northampton, MA) at 37 ℃ or 25 ℃. Prior to performing the ITC experiments, the RNA aptamers were denatured at 90 ℃ for 5 minutes and slowly refolded at 23 ℃ for 30 minutes. The RNA and the solutions containing binding partners were degassed at 20 ℃ for 5 minutes using the VP-ITC ThermoVac accessory (pulling a vacuum of 28.4 inches of mercury). A 300 µl solution containing one of the binding partners was injected from the syringe in 10-µl portions for 6 sec durations with each injection, and at 5-10 minutes intervals between the injections for equilibration. Dilution experiments were performed in the absence of one of the binding partners in the cell compartment of the ITC instrument. After each injection, the generated heat

of the binding reaction was recorded. ITC binding curves were analyzed by using the MicroCal Origin software package.

RESULTS AND DISCUSSION

Determination of molar extinction coefficient

To have a more convenient means of determining the concentrations of PD173955N in solution, the molar-extinction coefficients were calculated. PD173955N was dissolved in chloroform and transferred into a microcentrifuge tube. The chloroform was evaporated and the mass of the tube was recorded. The dried PD173955N in the tube was dissolved in 50% ethanol and 50% DMSO. When the absorbance between 200-800 nm was read using the UV-Spectrophotometer, two peaks were observed (Figure 4, Page 37). Prior recording all the readings, solution of 50% ethanol and 50% DMSO was used as reference. The UV-Spectrophotometer unit automatically subtracted the reference readings. One peak was observed at 299 nm and the other at 354 nm. The molar extinction coefficients for both wavelengths were calculated and they are 8525 and 16504 $M^{-1}cm^{-1}$ respectively. This experiment was repeated twice and the same molar extinction coefficients for PD173955N were obtained. These values were used later to estimate the concentrations of PD173955N.

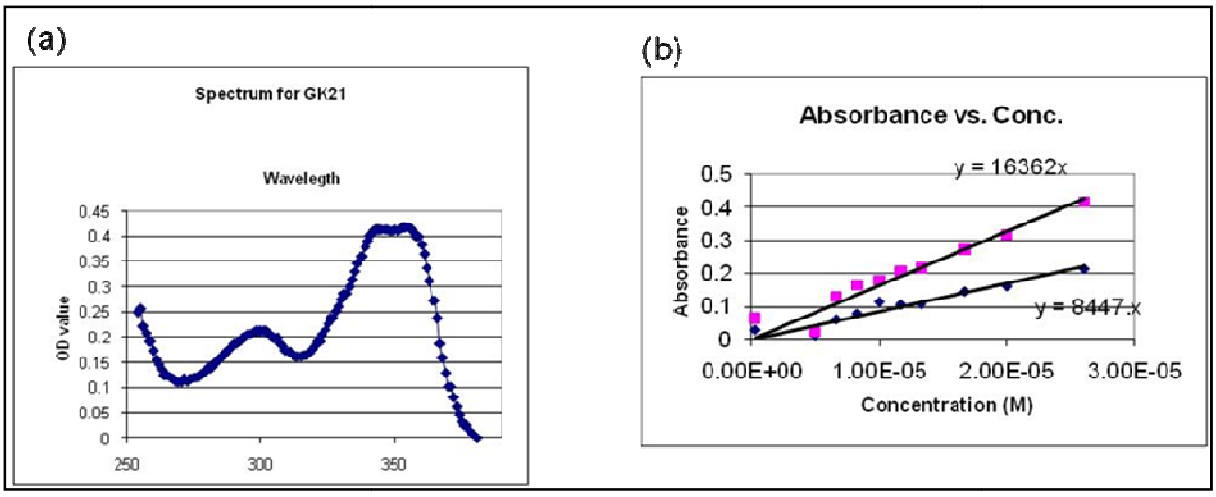

Figure 4: **UV absorption spectrum of PD173955N.** (a) A UV-vis absorption scan of the PD173955N in 50% ethanol and 50%DMSO measured from 200-800 nm. The molar extinction coefficients were calculated by graphing a known concentration of PD173955N in 50% ethanol and 50% DMSO against the collected absorbance readings at 299 and 354 nm.

Selection of RNA aptamers

SELEX was used to select RNA aptamers with high affinity for PD179355 from an RNA library of 100mers that contained a random region of 56 bases. Because PD173955 is a very small molecule, streptavidin beads were used to capture the PD173955B-RNA complex on the filter. The number of unique RNA molecules in round one was ~10^{14}. ITC was used to determine the K_D of the initial pool for the mathematical simulation. The ITC data showed that there was no significant difference in the profiles from titration of PD173955N into the initial RNA pool or into the buffer (Figure 5a and b, Page 39). There was no significant K_D measured by ITC therefore the initial K_D of the RNA pool for PD173955N was arbitrarily estimated to be 50 mM (Figure 5, Page 39). The background binding of

RNA to the filter and the streptavidin beads was determined experimentally as 3% of the total RNA. Using these three parameters, the simulation program returned the least number of rounds of selection necessary to select the aptamer if the initial concentration ratio was set to be 2 μM PD173955B and 1 μM RNA. With the reduction in the target concentration set to 10% in each round, the model predicted that at least 5 selection rounds would be necessary to achieve optimal selection (Figure 6a, Page 41). These conditions were used for S570. For the S569, the same concentrations were used, but the reduction of the target concentration was set to zero, and the simulation model predicted that at least 7 rounds were necessary (Figure 7a, Page 43). When these two figures are compared, the mathematical simulation modeling suggested that increased pressure on the selection should help reduce the number of necessary rounds.

In the S570 12 positive rounds and 2 negative rounds were completed before the PCR product was cloned and sequenced. After 8 positive rounds, the amount of RNA bound has increased to 14% (Figure 6b, Page 41). After four more positive rounds and one negative selection round there was no increase in the fraction of captured potential RNA aptamers (Figure 6b, Page 41).

The simulation model predicted that only 5 selection rounds were necessary to reach a maximum percent of the RNA bound. It can be seen on the Figure 6b (Page 41) that the maximum percent of RNA bound was reached after 8 rounds.

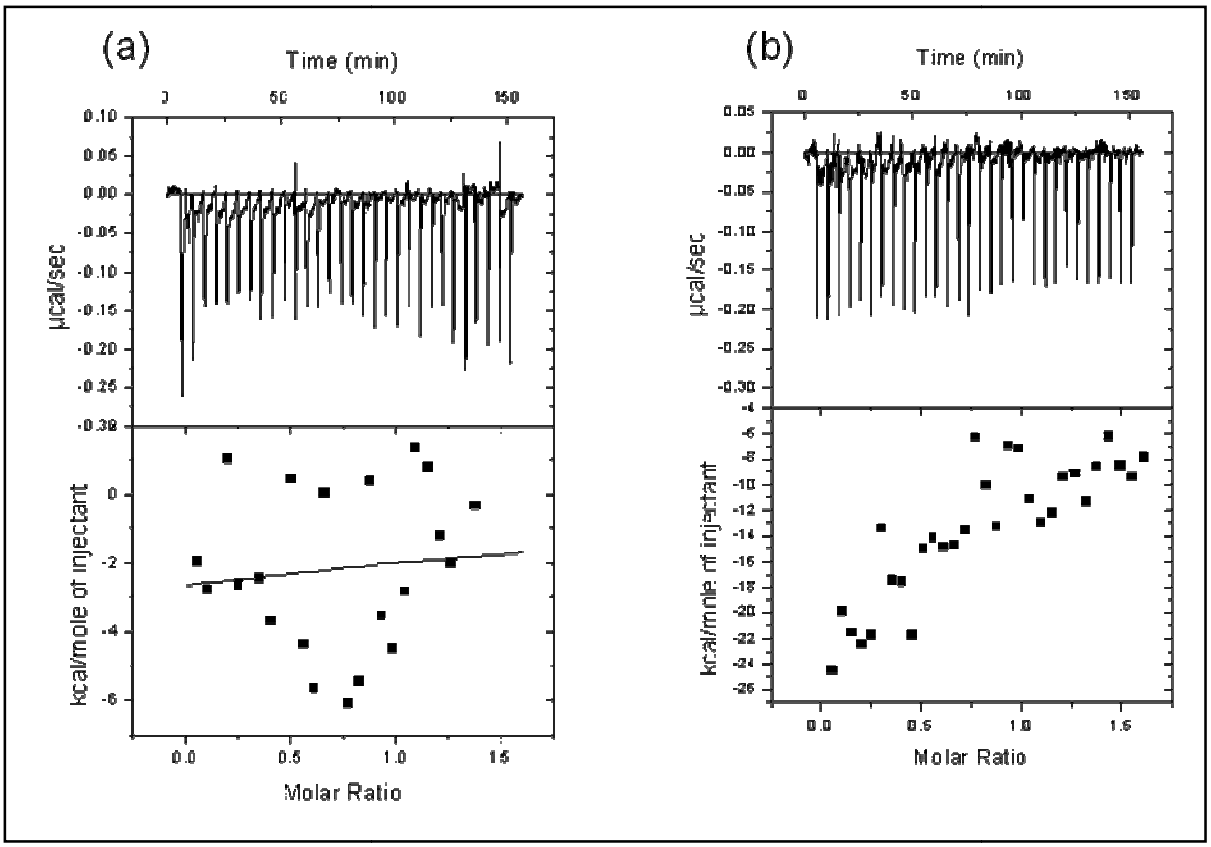

Figure 5: ITC titration of PD173955N with the initial random RNA pool. Shown is (a) the titration of 46 µM PD173955N with the 6.5 µM random RNA pool in buffer A (13.5 mM NaCl, 150 mM KCl, 0.22 mM Na_2HPO_4, 0.44 mM KH_2PO_4, 100 µM $MgSO_4$, 120 nM $CaCl_2$, 120 µM $MgCl_2$, 20 mM HEPES, 6 mM glutathione, pH 7.25) at 37°C, and (b) the PD173955N dilution into buffer A. The data in (b) was subtracted from the data that was obtained in (a) to calculate the K_D. The K_D, calculated by the Origin software, was 50 mM. The upper sections of both graphs represent raw ITC profiles obtained. The lower section of the graph in (a) shows the subtracted data, and in (b) shows the raw ITC data.

The PCR amplified pool from positive round 12 was cloned. Fifty clones were picked, grown overnight and their plasmids extracted and sent for sequencing. Of the fifty picked clones only 43 clones contained DNA inserts. All but one clone were shorter in the randomized region compared to the starting pool. The shortening may have been due to deletion during PCR amplification because of strong stem-loop

structures where the DNA polymerase was not capable of amplifying. Another possibility is that melting of the RNA molecules was not complete because of the low incubation temperature during reverse transcription. During the SELEX experiments it was observed on the gel images that the size of the PCR amplicon and the transcribed RNA was decreasing as the number of rounds increased.

In S569, 12 positive and 4 negative selection rounds were performed. According to the simulation model, seven rounds would be necessary to reach a maximum fraction of the RNA aptamers bound. The data obtained experimentally are shown in the Figure 7b (Page 43). In the eighth round of the SELEX experiment, 25% of the RNA pool bound to the target. Further rounds failed to preserve the high percentage of the RNA pool bound to the PD173955B. The percent bound in the 12^{th} round was about the same that was observed in S570.R12.

Because the highest percentage bound was observed in round 8, it was decided to clone the PCR product obtained after the reverse transcription of the bound RNA in round 8. One hundred clones were picked and sequenced. Out of the 100 picked clones 96 sequences were obtained. The random derived regions of the obtained sequences are listed in Table 3 (Page 51). As can be seen from the table most of the sequences have the full length random region, unlike in S570 (Table 1, Page 47) where the majority of the sequences were truncated.

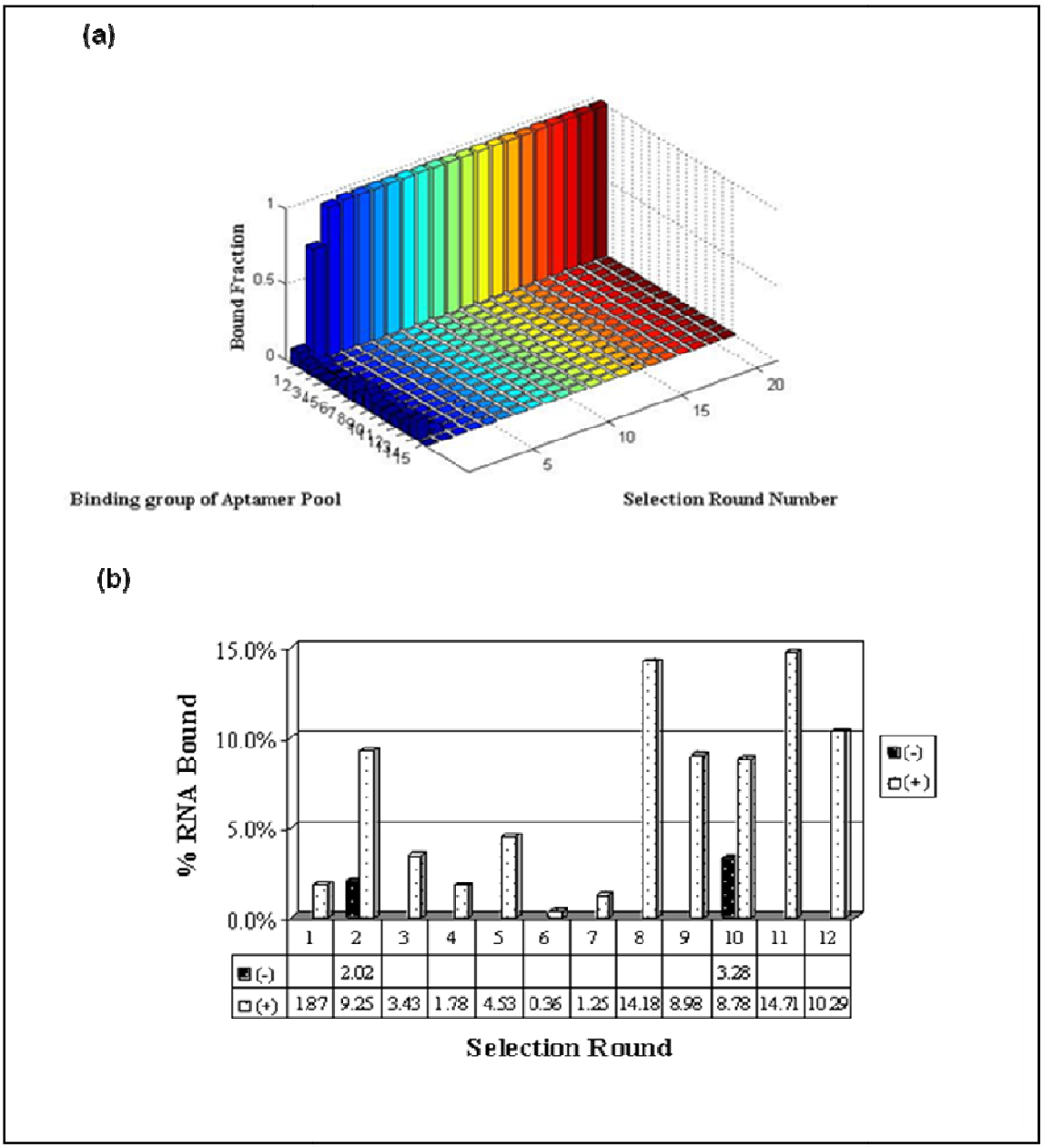

Figure 6: Computational prediction and progress of S570. (a) Computational analysis of S570 and (b) progress of S570. The 3D white bars represent positive selections, and the black bars represent negative selections. The percentage of RNA bound was plotted against the selection round number. The table below the graph in (b) shows the numerical values obtained in each round.

Alignment of the sequences from both SELEX experiments revealed a number of repeated sequences in each SELEX experiment (Table 1, Page 47 and Table 3, Page 51). Two small families of putative aptamers were obtained. All identified sequences except one had a decreased number of nucleotides in the randomized region in S570. Four clones in S570 that displayed identical sequences (Clone 10) were classified in the first family. S570.R14.C32 RNA is a member of family one except it contains a single base insert within the random region (Table1, Page 47). The same sequence was repeated six times in S569 (S569.R8.C43). The two most stable secondary structures predicted by M-fold of the S570 R14.C32 RNA are shown (Figure 8a, Page 44). The second smaller family was mostly present in S569 (S569.R8.C15). It has the same sequence as S570.R14.C47. These were classified as the second family of aptamers. The consensus sequences of the family one and the family two aptamers are not related to that of the reported ATP RNA aptamer (Sassanfar and Szostak 1993; Dieckmann, Suzuki et al. 1996; Vaish, Larralde et al. 2003). The sequence and the secondary structure of the ATP RNA aptamer predicted by M-fold is shown in Figure 8b (Page 44). As it can be seen on Figure 8a and b (Page 44) the aptamer representing family one of the sequence, and its predicted secondary structure is different from that of the ATP RNA aptamer. Clones 23, 25, and 31 also had identical sequences, representing a second family of aptamers. The binding affinities of these clones were determined using ITC.

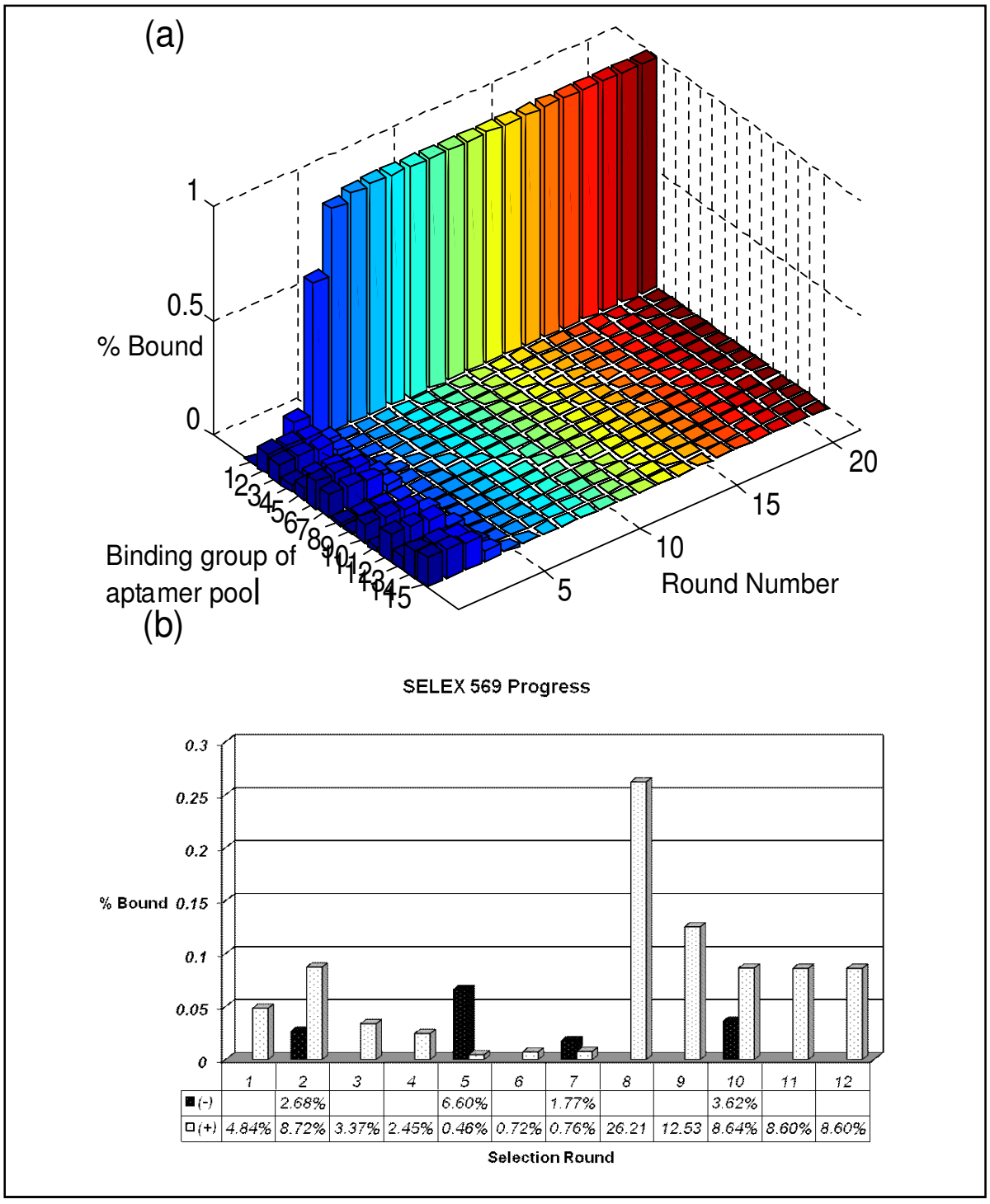

	1	2	3	4	5	6	7	8	9	10	11	12
■(-)		2.68%			6.60%		1.77%			3.62%		
□(+)	4.84%	8.72%	3.37%	2.45%	0.46%	0.72%	0.76%	26.21	12.53	8.64%	8.60%	8.60%

Figure 7: Computational prediction and progress of S569. (a) Computational analysis of S569 and (b) progress of S569. The 3D white bars represent positive selections, and the black bars represent negative selections. The percentage of RNA bound was plotted against the selection round number. The table below the graph in (b) shows numerical values obtained in each round.

Determination of dissociation constants of putative RNA aptamers

The dissociation constants of the selected putative RNA aptamers for PD173955N were determined by isothermal calorimetry (ITC) and they varied from 2-11 μM (Table 2, Page 49). The aptamers from family one had K_Ds ranging between 2-3 μM for PD173955N, and the aptamers from family two had K_Ds around 11 μM (Table 2, Page 49). S570.R14.C32RNA, with a dissociation constant of 2 μM, was chosen for further studies, because it gave the lowest dissociation constant. Representative ITC data obtained for S570.R14.C32 is shown (Figure 9a, Page 45).

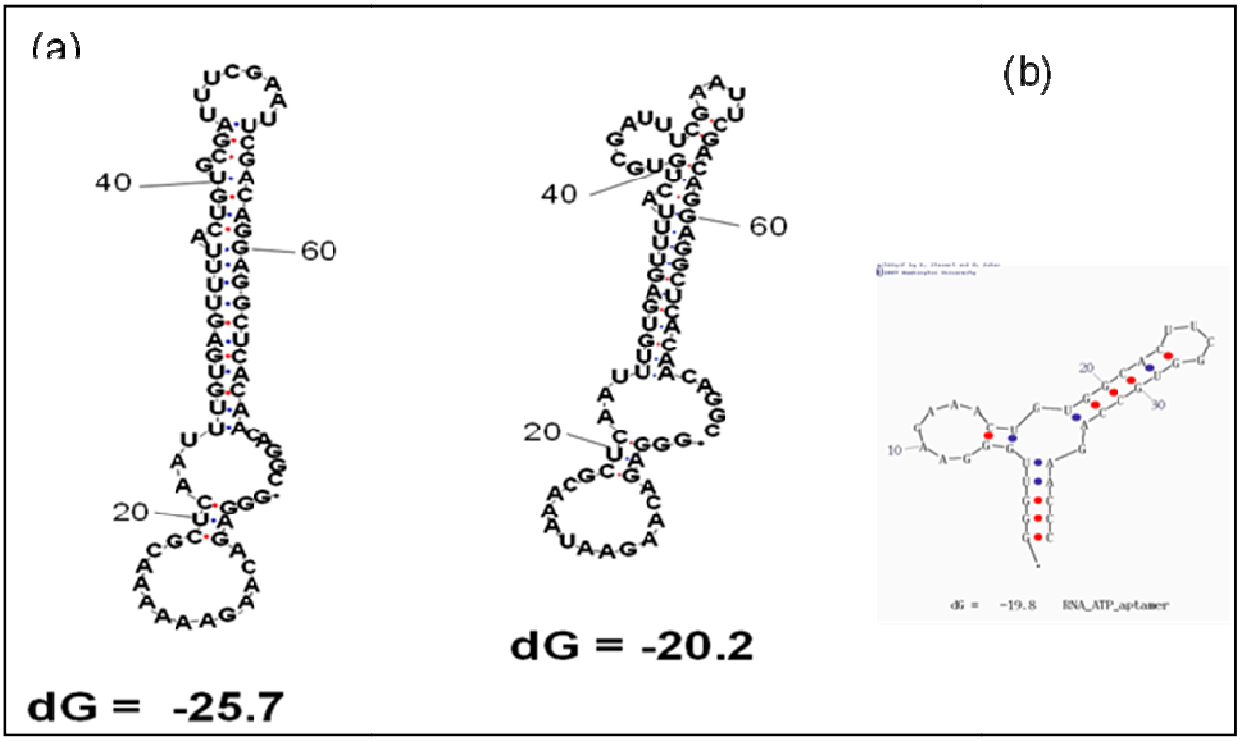

Figure 8: RNA secondary structures predicted by the M-fold. Shown are (a) the two the most stable structures of S570.R14.C32RNA, and (b) the structure of the ATP RNA aptamer. All structures were determined by M-Fold.

Binding of S570.R14.C32 to ATP and adenosine using ITC was checked under similar ITC conditions as this putative RNA aptamer was tested with PD173955N. The aptamer did not show any binding under the conditions that were used, and from the ITC data obtained it was not possible to calculate a K_D for ATP and adenosine (Figures 10 and 11). The result is consistent with the observation that the secondary structure of the aptamer does not resemble any part of the RNA ATP aptamer (Figure 8, Page 44).

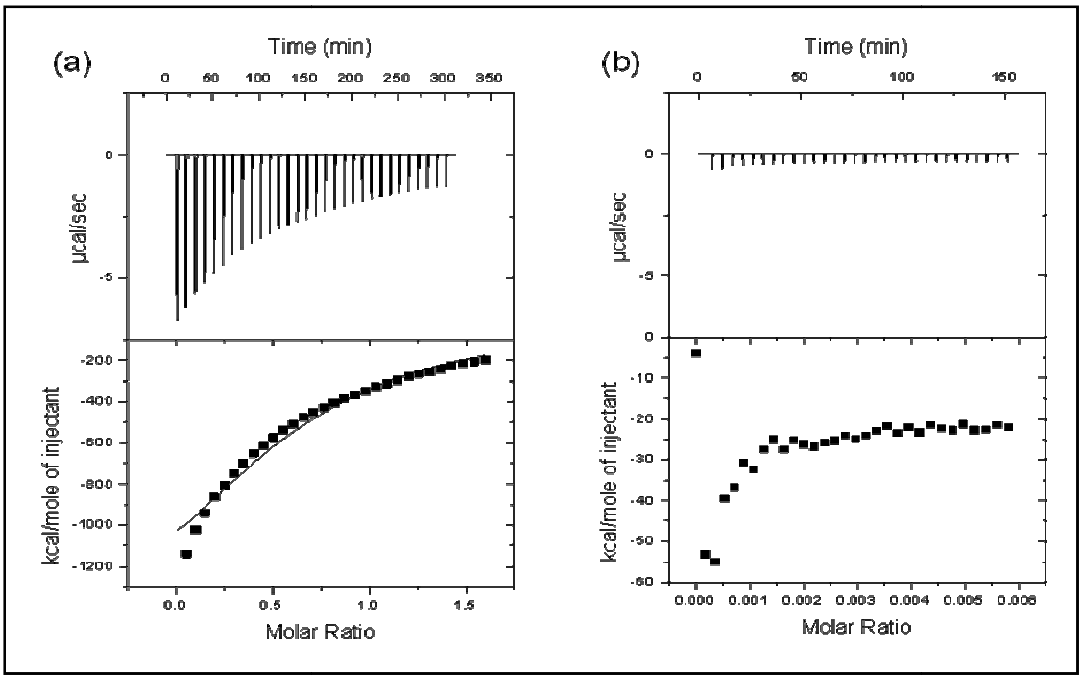

Figure 9: Determination of thermodynamic parameters by ITC. Shown is (a) the titration of 28 µM S570.R14.C32 RNA into a solution containing 4 µM PD173955N after the reference data was subtracted, (b) the reference data with PD173955N titrated into buffer. This experiment was repeated five times with similar results each time.

We wanted to further test the specificity of the S570.R14.C32 RNA aptamer to other compounds that are similar in structure to PD173955. Using ITC the binding of 4-[(3-Bromophenyl)amino]-6-propionylamidoquinazoline (PD174265, Calbiochem) to the full length aptamer S570.R14.C32 RNA was determined. PD174265 is a member of the pyrido[2,3-d]pyrimidine family of compounds which are Src family kinase inhibitors (Tulasne, Judd et al. 2001) and like PD179355N is not very soluble in water based buffers. The dissociation constant of S570.R14.C32 for PD174265 is 20 µM (Figure 12, Page 50; Table 2, Page 49). Although a Kd was determined by the software, the ITC data for PD174265 and S570.R14.C32 does not show evidence of a titration. This suggests that S570.R14.C32 RNA aptamer does not bind PD174265.

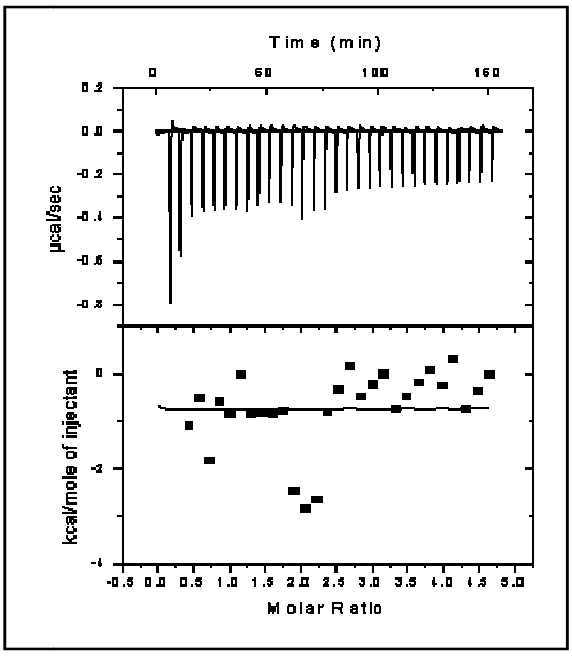

Figure 10: ITC titration of ATP with S570.R14.C32RNA. Shown is a titration of 100 µM ATP with µM S570.R14.C32RNA in 300mM KCl, 20 mM HEPES, 5 mM $MgCl_2$, 5% DMSO, pH 7.5 at 37 °C, after the data for separate titration of ATP dilution into buffer was subtracted. The analyzed data on the bottom half of the graph shows no binding

S570.R14.C32 RNA to ATP under these conditions. This experiment was repeated twice with similar results each time.

Name	No.	Random Region Sequence					
		....|....|	....|....|	....|....|	....|....|	....|....|	...
		5	15	25	35	45	
48	1	----------	-----ATCAA	CACAAGCCTC	ACGAAGCGGC	ACGTCA----	---
47	1	----------	---ATCAAAA	CACAAAGAGG	ACTCACAAAA	CA--------	---
45	1	----------	AAACGAACGA	AACAAACAGA	AGAGTCACA-	----------	---
46	1	----------	-------GAT	AGCAACAGAA	TCTCACAAGA	----------	---
44	1	----------	----------	--TG------	----------	----------	---
42	1	----------	-------TAA	CACGAGGCTA	ACAA------	----------	---
41	1	----------	----------	-------GGA	AGAAA-----	----------	---
43	1	----------	---ATCGCAA	TACGAGGTTC	ACAAAAT---	----------	---
40	1	----------	----------	--TGGTTAA-	----------	----------	---
39	1	----------	-----CAGCA	CACGAACAGA	AGACACACAC	A---------	---
38	1	GCGACAAACC	AGAGAACACG	AGCAGACAGG	GGAGAGCAAA	CAGTCAAGAA	AGG
37	1	----------	-----GTACT	CACATAAACT	TTATCGATT-	----------	---
36	1	----------	----------	-------GGA	----------	----------	---
34	1	----------	-------TGT	CA--------	----------	----------	---
33	1	----------	-------CAA	CGCACGGGAT	A---------	----------	---
32	1	----------	TTCGAAATCG	CACAGTA-AA	ACTCACAAA-	----------	---
31	2	----------	--------TC	AACAGTG-AA	ACTCACATTA	ATCATT----	---
28	1	----------	---------A	AACAGGCGAT	TCACGATTAA	CA--------	---
27	1	----------	------AAAG	AACAA-CAGA	AAGACCC---	----------	---
26	1	----------	------CCCA	AACAA-AAGA	GCATCACAAA	----------	---
25	2	----------	TTGCGGACAA	AACGATGGAA	ACTCAC----	----------	---
23	2	----------	----TCACGC	AACAAAGAGA	ACACACAAG-	----------	---
21	1	----------	-------TCA	GTCAGTCCAC	AATCTTT---	----------	---
20	1	----------	--TCATCCTC	AACAA-CATA	GACTCAAAAA	----------	---
19	1	----------	----------	--GGGACAAA	AAAGGACG--	----------	---
18	1	----------	----------	--C-------	----------	----------	---
17	1	----------	TAACTCAC-A	ATCGAAAACA	AA--------	----------	---
16	1	----------	-TGAGGGACT	CGTAGTCCGT	TTAAACAAGT	----------	---
15	1	----------	--------CC	AACAATCACA	ATGACCGA--	----------	---
11	1	----------	----------	---AG-----	----------	----------	---
10	4	----------	--TTCGAAAT	CGCACAGTAA	ACTCACAAA-	----------	---
09	1	----------	-TCAACATTA	AACAAGAGGA	TCAC------	----------	---
08	1	----------	---AGGTACT	CACATCAATT	CTT-------	----------	---
05	1	----------	------TTCA	AACACGA-AA	ACTCAC----	----------	---
04	1	----------	---ATCAAAG	CACAAAGAGG	ACTCACAAAA	CA--------	---
03	1	TCCGACTGTC	CGACGGATAG	CACACAAACT	----------	----------	---
02	1	----------	-------TCT	CACGTTTTCG	CTTAGTT---	----------	---

Table 1: The sequences of 43 clones from the 12th round of S570. Under “Name” is the sequence number, and under “No” is the number of times the sequence is repeated. The primer sequences are not shown.

If the structures of PD173955N and PD174265 are compared, it can be seen there are some similarities and crucial differences between two of them (Figure 2b and c, Page 26). PD174265 is a smaller compound then PD173955N.

They both contain three benzene rings that are spaced similarly and have a purine moiety in the main part of the molecule. But, otherwise their structures are different. For example, the bromobenzene ring that is further away from the purine part of the molecule in PD174265 has a than it is in PD173955. These large differences in structure are consistent with the observation that the aptamer binds PD173955 and not PD174265.

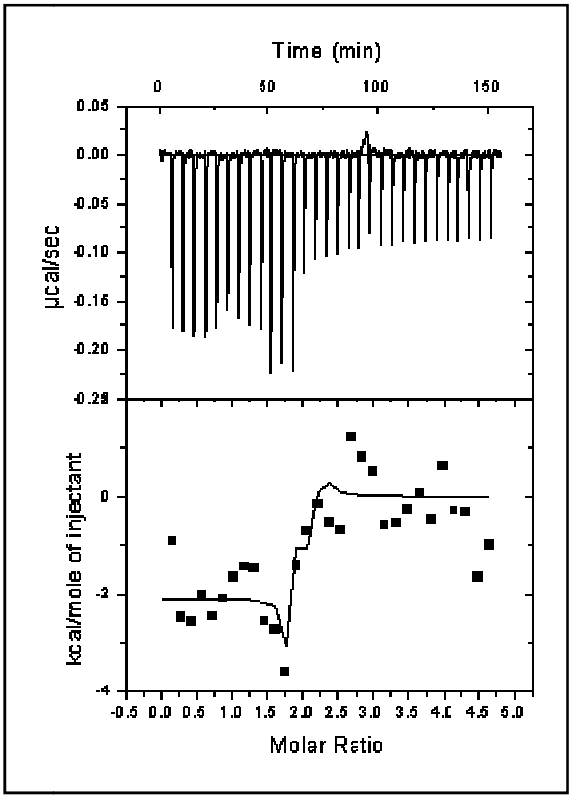

Figure 11: ITC titration of adenosine with S570.R14.C32RNA. Shown is the titration of 100 µM adenosine with 8 µM S570.R14.C32RNA in 300mM KCl, 20 mM HEPES, 5 mM $MgCl_2$, pH 7.5 at 37 °C after the data for separate titration of adenosine into the buffer was subtracted. The data shows no binding of S570.R14.C32RNA to adenosine under these conditions. This experiment was repeated twice with similar results each time.

Sequence No.	PD173955N Dissociation Constant (μM)	PD174265 Dissociation Constant (μM)	
SELEX570.R14.C32	1.2± 0.8	20	Family I
SELEX570.R14.C10	2.5		Family I
SELEX570.R14.C32T2	1	40	
SELEX570.R14.C10T1	57000		
SELEX570.R14.C47	26		Family II
SELEX570.R0	50000		

Table 2: Dissociation constants of the tested aptamer sequences determined by ITC.

During the SELEX experiments, the biotin/streptavidin system was used to capture the RNA/PD173955 complex. The biotin part of PD173955B was bound to the streptavidin binding pocket (Figure 2a, Page 26). If the aptamer pools were binding to the biotin part of PD173955B then the RNA/PD173955B would not been captured by the streptavidin. The S570.R14.C32 RNA aptamer does not bind ATP or adenosine under ITC conditions tested. PD173955 is an ATP analog and the purine part of the molecule resembles the structure of the adenosine (Figure 2d, Page 26). Adenosine has nitrogen that could interact with the PD173955N aptamer, but the ITC data does not show binding of adenosine to the S570.R14.C32 RNA aptamer, therefore the nitrogen does not have a significant role in binding to the aptamer. The purine part of the molecule does not have a benzene ring attached to it, but from the structural comparison, the benzene ring is not very important in binding of PD173955N with the aptamer. It is very difficult to determine which parts of the target molecules the selected aptamer binds, because the RNA aptamer makes a number of contacts with PD173955N. Most aptamers are believed to bind

their targets through the induced fit model. The lack of aptamer binding to ATP and adenosine was confirmed by ITC. The RNA footprinting data suggests that binding of adenosine with the S570.R14.C32 RNA aptamer does not protect the aptamer from RNase ONE cleavage in the region where it is protected when PD173955N is present (Figure 16a and b, Page 64).

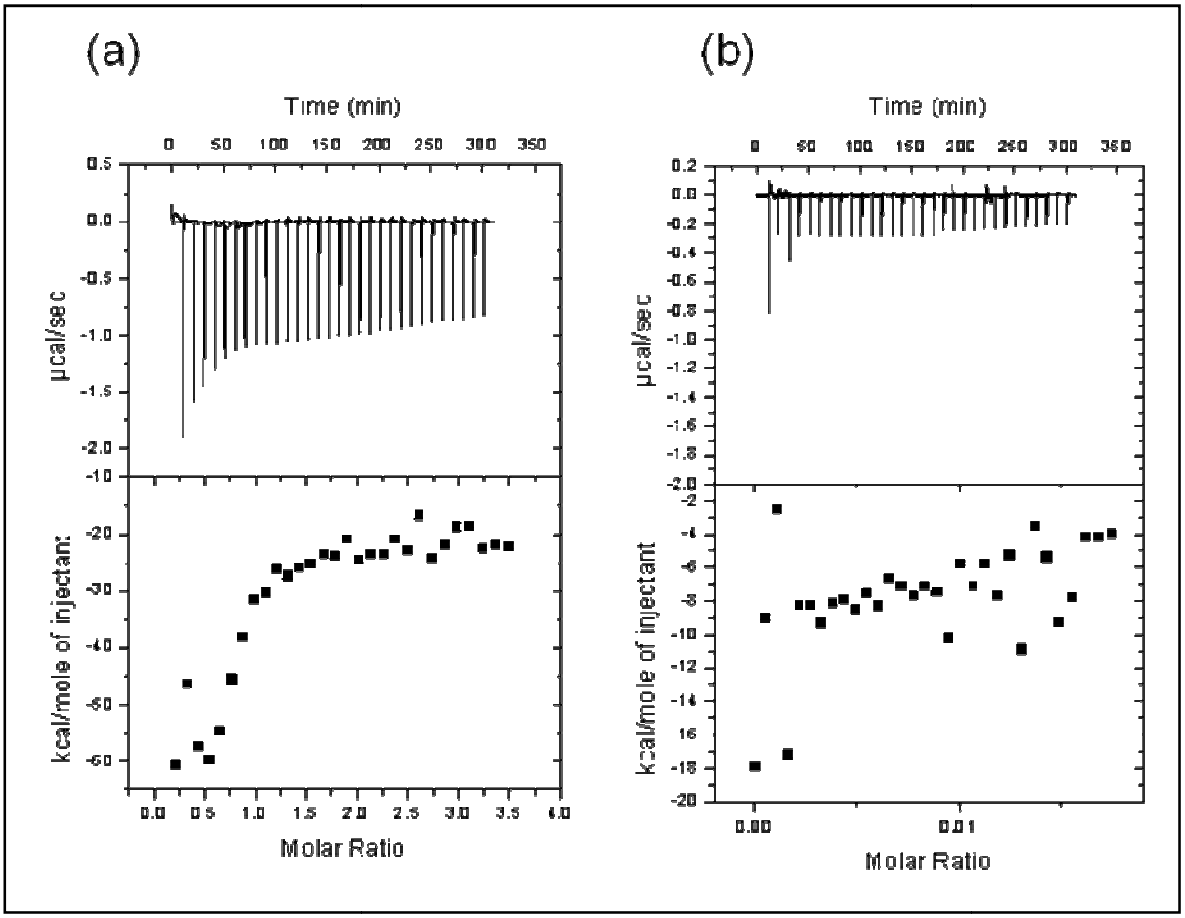

Figure 12: ITC titration of PD174265 with S570.R14.C32RNA. Shown is (a) a titration of 75 µM PD174265 with 5 µM S570.R14.C32RNA in 300mM KCl, 20 mM HEPES, 5 mM $MgCl_2$, 5%DMSO, pH 7.5 at 37°C , and (b) after the data for PD174265 dilution into buffer was subtracted. The K_D, calculated by the Origin software was 20 µM. This experiment repeated twice with similar results each time.

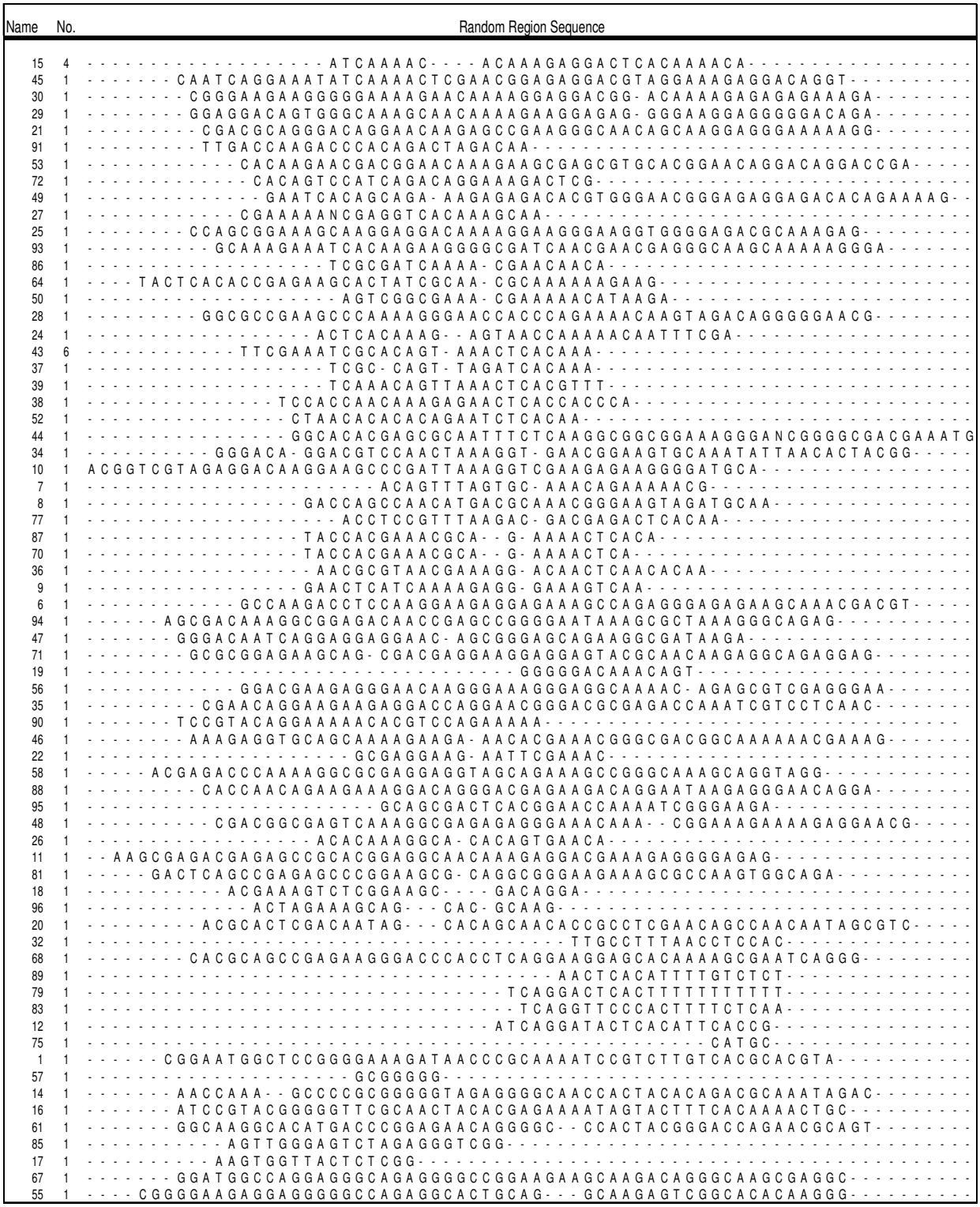

Table 3: The sequences of 96 clones from the 8th round of S569. Under “Name” is the sequence number, and under “No” is the number of times the sequence is repeated. The primer sequences are not shown.

CONCLUSION

The SELEX method is an efficient way to generate an RNA aptamer to a small compound. The conditions used in the two SELEX experiments reported here can be used to select RNA aptamers to a number of small compounds. The mathematical simulation model can be used as a guide to set the initial SELEX conditions. Also, it can be used to approximate the number of the selection rounds that one needs to do before seeing an increase in binding of the RNA pool. The simulation modeling was useful because it recommended selection conditions that resulted in two successful SELEX experiments.

It is very interesting that oligonucleotides with the same sequences were present in both SELEX outcomes. The aptamers that belong to the second family that were mostly found in S569 might have been eliminated when the selection pressure was applied in S570. The ITC data shows that the aptamers that belong to the second family have 5-10 times lower affinity for PD173955 compared to the aptamers that belong to family I.

The next step in development of the aptamer is to minimize the size of S570.R14.C32 RNA aptamer. Even though the size of the aptamer was reduced through SELEX from 100 nucleotides long to a 78 nucleotides, it is desired to further reduce its size to eliminate segments that are not part of the aptamer. The regions of the aptamer involved in the binding also need to be characterized. The M-fold software predicted a number of different secondary structures of the selected RNA aptamer and the two most stable structures are shown in the Figure 8 (Page 44). In

the next section of this thesis the truncation and characterization of the selected aptamer will be described.

CHAPTER 3: CHARACTERIZATION OF THE RNA APTAMER TO PD173955N THROUGH RNA FOOTPRINTING ANALYSIS

INTRODUCTION

In chapter 2 it was mentioned that multiple secondary structures were predicted by M-fold software (Figure 8, Page 44). In order to predict the region or regions of the RNA aptamer that bind PD173955N it was necessary to determine which secondary structure was correct. RNase ONE footprinting analysis of the selected aptamer was done to determine which predicted M-fold structure best represents the data obtained through footprinting analysis.

In chapter 1 the reasons were given why it was necessary to minimize the size of the selected aptamer, which include higher specificity and affinity of the PD173955 aptamer to the target, and being able to chemically synthesize the RNA aptamer. Also it is beneficial to remove non binding conformations, of the RNA aptamer which can be achieved through size reduction. Minimization of the aptamer can be done by using a few methods. Some of methods are: boundary studies, enzymatic probing and site directed mutagenesis (Pendergrast, Marsh et al. 2005).

In this chapter the results will be described of the studies that were used to characterize the selected aptamer and to minimize its size without loss of affinity for the target. The S570.R14.C32 RNA aptamer produced the best binding constant for PD173955N, and it was chosen for further analysis and modification. By the use of

RNase ONE probing, the part of the RNA that is making a contact with the PD173955N was predicted. Unlike proteins, PD173955N is a small compound and makes fewer contacts with the aptamer, which makes it more difficult to determine the binding regions (Sayer, Ibrahim et al. 2002).

MATERIALS AND METHODS

5'-end labeling of RNA and purification

Dephosphorylation of S570.R14.C32 RNA was carried out at 37°C for 30 minutes in a 50 µl reaction that contained 50 mM Tris-HCl 1 mM $MgCl_2$, 0.1 mM $ZnCl_2$, 1 mM spermidine, 0.04 U/µl alkaline phosphatase (Promega, Madison, WI), (pH 9.3) and 0.02 mM of RNA. An additional 0.04 U/µl alkaline phosphatase was added and the reaction was incubated for 30 more minutes. The RNA was phenol/chloroform extracted and ethanol precipitated as described previously (Chapter 2). One nmole of the RNA was 5'end labeled with 20 units of T4 polynucleotide kinase (Promega, Madison, WI) and 100 µCi [γ-^{32}P]ATP (MP Biomedicals, Solon, OH) in 70 mM Tris-HCl 10 mM $MgCl_2$, 50 mM DTT (pH 7.6) for 1.5 h at 37°C in 50 µl. The reaction was stopped by adding EDTA to a concentration of 19.3 mM. The RNA was ethanol precipitated and purified through a denaturing PAGE gel as described previously (Chapter 2).

RNA footprinting Assays

Determination of enzymatic probing conditions

The necessary RNase ONE (Promega, Madison, WI) incubation times were determined by cleaving 0.5 µM RNA for 2, 5, and 10 minutes with $4.76x10^{-4}$ U/µl RNase in a 10 µl reaction mixture containing 300 mM KCl, 5 mM $MgCl_2$, 20 mM HEPES, 5% DMSO, pH 7.5. A mild alkaline hydrolysate was generated by incubating 0.5 µM RNA at 95 ℃ for 2, 5, and 10 min in *10 µl 50 mM Na_2CO_3, pH 9.3. The G-residue ladders were generated by digestion of 0.5 µM RNA for 2, 5, or 10 minutes at 55 ℃ in 7 M Urea, 20 mM sodium citrate, 1 mM EDTA, pH 4.4 with 2 U/µl RNase T1 (Promega, Madison, WI) in 10 µl.

Enzymatic probing and electrophoresis

Samples containing 0.5 µM of gel-purified, 5'end-labeled, and renatured RNA in 300 mM KCl, 5 mM $MgCl_2$, 20 mM HEPES, 5% DMSO, pH 7.5 were incubated with PD173955N or adenosine ranging from 0 to 15 µM at 23 ℃ for 30 minutes in 5 µl. RNase ONE was added to the concentration of $4.76x10^{-4}$ U/µl and the samples were incubated for an additional 5 min at 37 ℃. All samples were brought to 47.5% formamide, 0.05% bromphenol blue, 0.05% xylene cyanol FF to stop cleavage. The samples were resolved for 30-45 min at 2000V at 55 ℃ through 8% or 10% polyacrylamide gels containing 7 M urea gels in TBE buffer. A partial alkaline hydrolysate of the RNA along with a G-residue ladder sample was run alongside a

series of footprinting analysis samples to aid in sequence identification. The dried gels were exposed to a Phosphor screen (GE Healthcare, Piscataway, NJ), which was read using the Typhoon 8600 Variable Model Imager (GE healthcare, Piscataway, NJ). The gel images were analyzed using Semi-Automated Footprinting Analysis software (SAFA) (Das, Laederach et al. 2005).

Measurement of Binding Affinities by ITC

See Chapter 2 (Materials and Methods)

RESULTS AND DISCUSSION

Preliminary RNA footprinting analysis was performed to determine the incubation time course of RNase degradation of the aptamer and the incubation time necessary to reach complete hydrolysis of RNA. After 10 minutes of hydrolysis of the RNA complete degradation was observed (Figure 13, Page 58). The G-residue ladder was obtained after incubating the RNA aptamer for 5 minutes with the RNase T1 which degrades single stranded RNA molecules at G residues. When the RNA was digested with RNase T1 for longer than 5 min, the higher molecular weight RNA fragments were not visible on the gel (Figure 13, Page 58), and 2.5 minutes incubation with the RNase T1 was sufficient to create the G-ladder. RNase ONE degrades single stranded RNAs to monomers and oligomers. Longer incubation times then 5 minutes with the RNase ONE did not produce any additional RNA

fragments from digestion of the RNA, when compared to incubation times of less than 5 minutes (Figure 13, Page 58). Based on this data all the enzymatic probing of the RNA aptamer with RNase ONE was done for 5 minutes using the conditions given in the Material and Methods (Chapter 3).

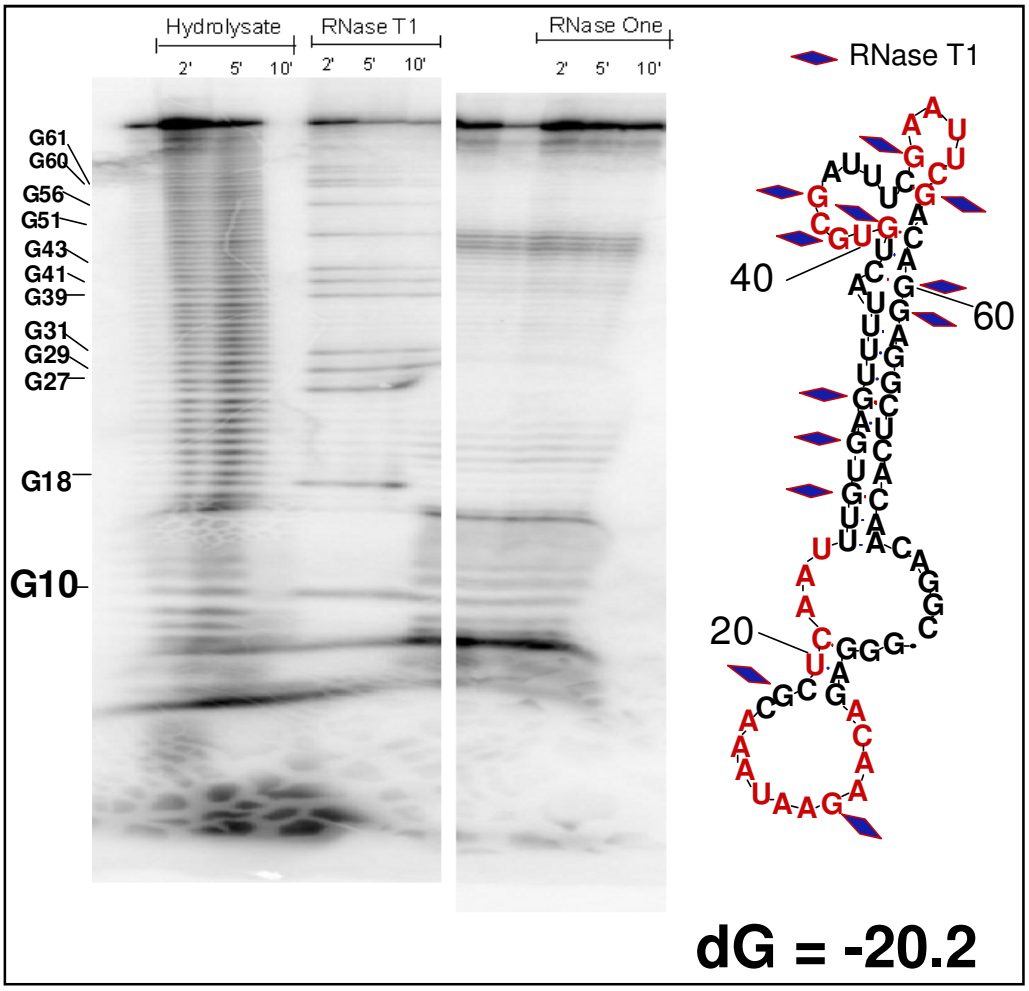

Figure 13: Enzymatic probing of S570.R14.C32 RNA. The gel image shows enzymatic probing of the S570.R14.C32 RNA. The first three lanes represent hydrolysis of RNA at 2, 5, and 10 minutes. The next three lanes represent RNase T1 digestion of RNA at 2, 5, and 10 minutes. The last three lanes represent RNase ONE cleavage of the RNA at 2, 5, and 10 minutes. Secondary structure of RNA aptamer: the blue diamonds represent RNase T1 digested nucleotides; the red colored letters represent RNase ONE digested nucleotides.

Structural analysis of the S570.R14C32RNA aptamer

Prediction of the first truncated aptamer

The first attempt to truncate the S570.R14.C32 RNA involved using the M-fold software to predict possible secondary structures and comparing their stabilities. Because the random region of the selected aptamer was capable of forming a strong secondary structure (Figure 14c, Page 60), it was decided to chemically synthesize the random region of S570.R14.C10T1. For the first truncation, the sequence was 5'-GCUCAAUUUGUGAGUUUACUGUGCGAUUUCGAA-3'. The extension T1 in the sequence name designates the first truncation tested. The first truncation yielded an aptamer that had a very low affinity to PD173955N (Figure 14a, b, and c, Page 60). The results from this study led to the design of the second truncated aptamer.

Prediction of the second truncated aptamer

As mentioned previously M-fold predicted multiple secondary structures of the putative aptamer S570.R14C32RNA (Figure 8, Page 44). Most predicted structures contained loops at both ends that were connected with a long stem. RNase ONE footprinting analysis was performed to determine which predicted structure was likely to be correct. Radioactive 5'-end labeled RNA was digested by the single stranded specific RNase ONE. The RNA footprinting data was analyzed from gel images using SAFA, a program that uses a peak fitting routine to determine which regions of the nucleic acid are degraded more in the test sample compared to the

reference. The extracted data were normalized such that the undigested RNA corresponded to zero.

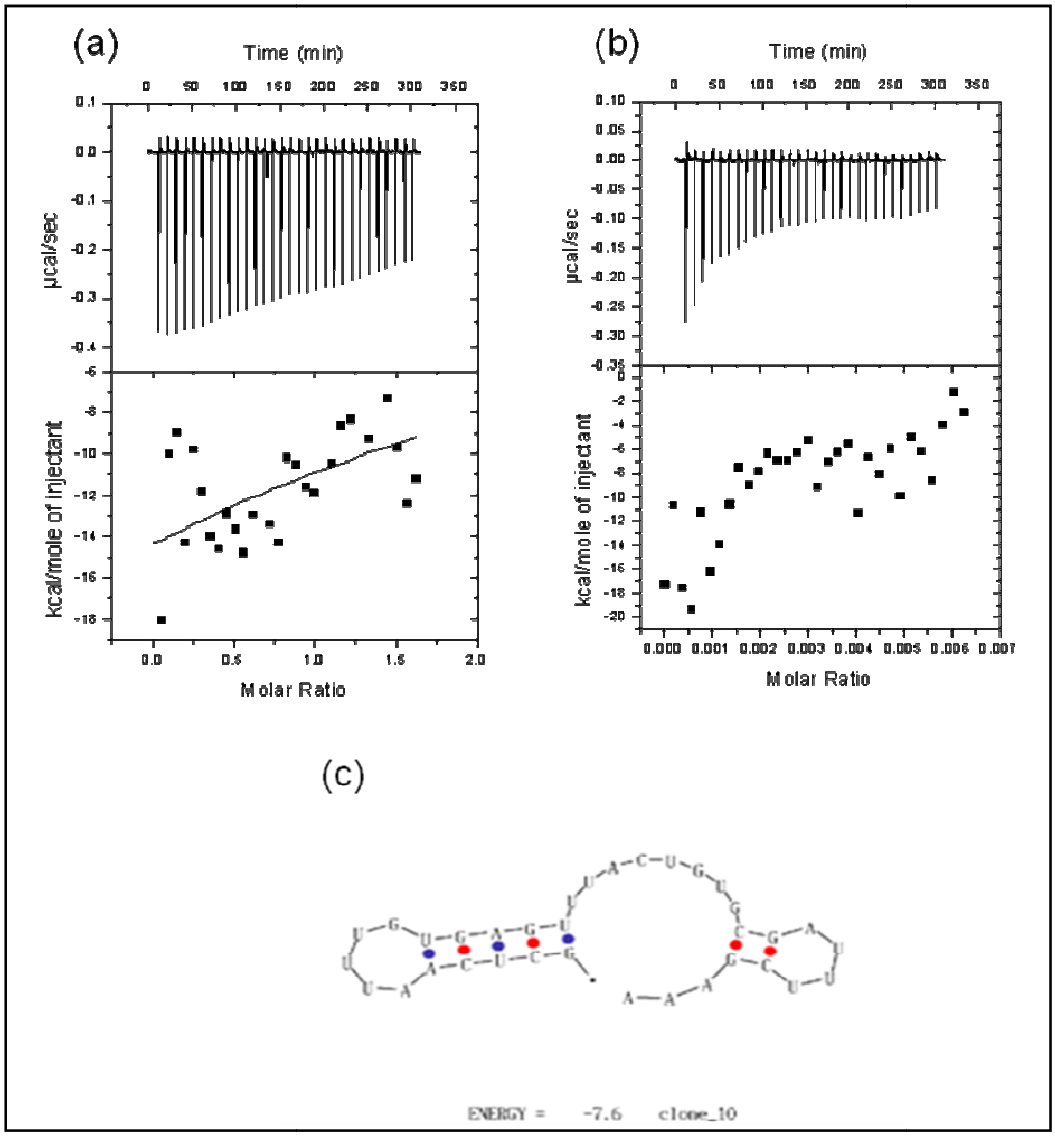

Figure 14: ITC titration of PD173955N with S570.R14.C10T1RNA and the M-fold predicted Structure. Shown is (a) a titration of 4 µM GK21 with 28 µM aptamer RNA after the data for the RNA aptamer dilution into buffer was subtracted, (b) The RNA aptamer titration into buffer. The K_D, calculated by the Origin software, is 57 mM, and (c) The secondary structure of the RNA aptamer predicted by M-fold. This experiment was done only once.

When the putative aptamer was incubated with different concentrations of PD173955N for 30 minutes prior to digestion with RNase ONE, nucleotides 50-60 were protected from RNase ONE cleavage at concentrations of 1 μM PD173955N and higher (Figure 15a, b, and c, Page 62). The region of the RNA that was protected from RNase ONE cleavage is circled on the predicted secondary structure by M-fold, and that structure had the lowest ΔG of all predicted secondary structures (Figure 8, Page 44). This result suggested that interaction of PD173955N with RNA protects the putative aptamer from RNase ONE digestion in the region of the predicted loop and that therefore PD173955N might bind within the loop region of the predicted RNA structure. The same experiment was repeated with adenosine instead of PD173955N and protection from RNase ONE within the same region was not observed (Figure 16a, b, and c, Page 64). This is consistent with the observation that adenosine does not bind the aptamer.

Based on the structural analysis just described, a truncated S570.R14.C32 RNA aptamer named S570.R14.C32T2 was synthesized that contained the loop region and part of the long stem of the S570.R14.C32 RNA aptamer. In order to stabilize the secondary structure four GC base pairs were added to the end of the stem. Using M-fold, one of the predicted structures of the truncated aptamer was the same as for this region in the full length putative aptamer (Figure 17, Page 66). This truncation reduced the size of the putative aptamer from 74 to 37 nucleotides long. The RNA sequence of S570.r14.c32T2 is: 5'-CGCGUUUACUGUGCGAUU

UCGAAUUCGACAGGACGCG-3'. The T2 extension in the name of the aptamer designates the second truncation.

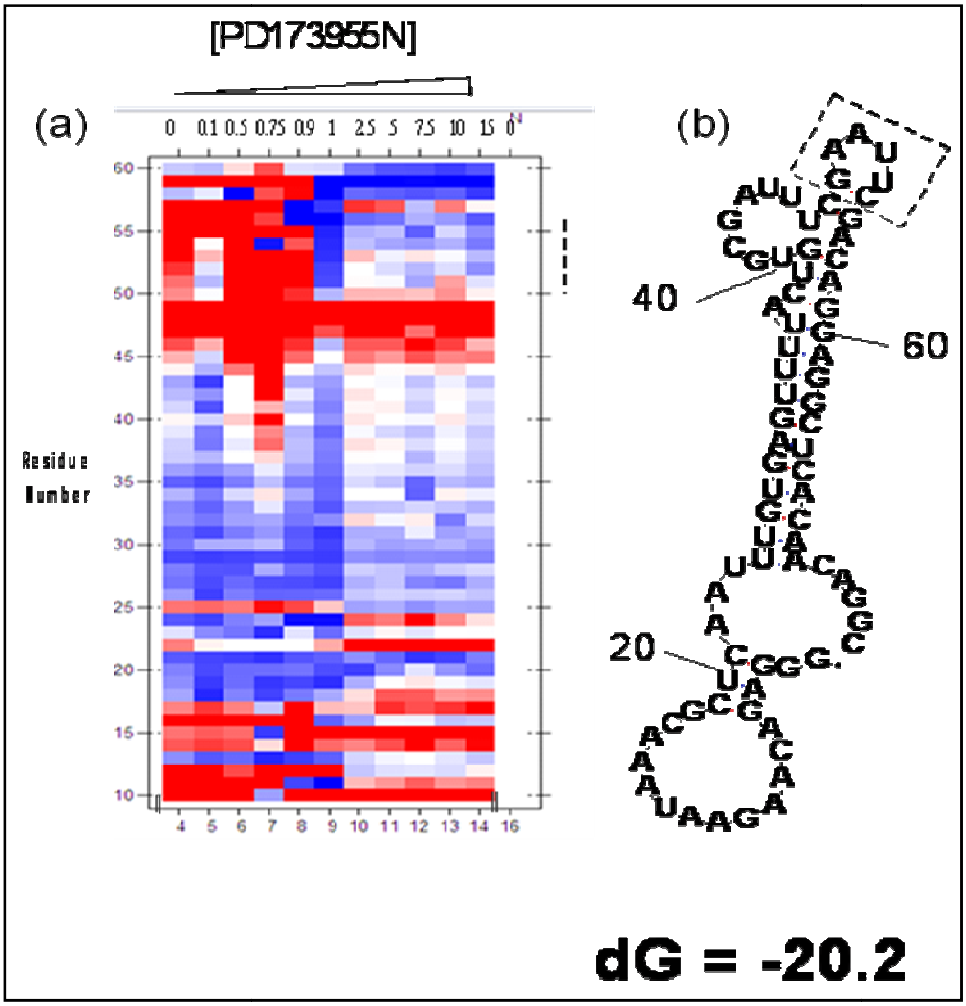

Figure 15: Enzymatic probing of S570.R14.C32 RNA. Enzymatic probing was performed by incubating 0.5 µM of 5' end labeled RNA aptamer with different concentrations of GK21, and probing it with RNase ONE in a 10 µl reaction mixture. The cleaved RNAs were run on a 10% PAGE denaturing urea gel. A partial alkaline hydrolysate, RNase T1 (G residue ladder) digest, and the undigested RNA aptamer were run to allow alignment with the known sequence for SAFA analysis. (a) the analyzed image using SAFA. The lanes that contained hydrolysate and the RNase T1 digest were removed from analysis. The data were normalized such that the undigested RNA "equals" zero. In this image the blue color regions show protection from RNase ONE digestion and the red color regions represent increased digestion. b) one of the secondary structures that corresponds to the data obtained and the region of interest is indicated by dotted lines. (c) the raw gel image. This experiment was repeated twice with similar results each time.

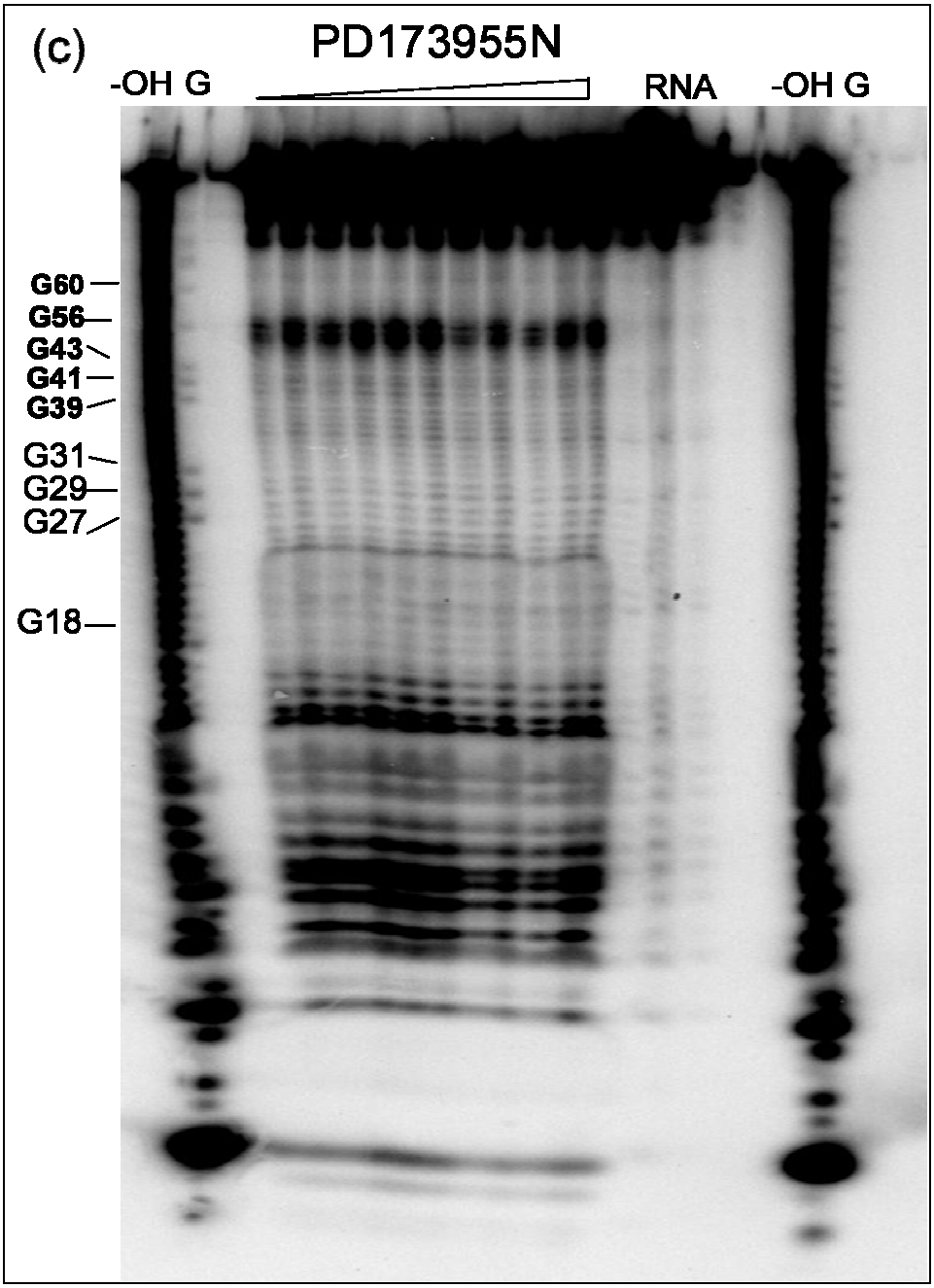

Figure 15: (continued)

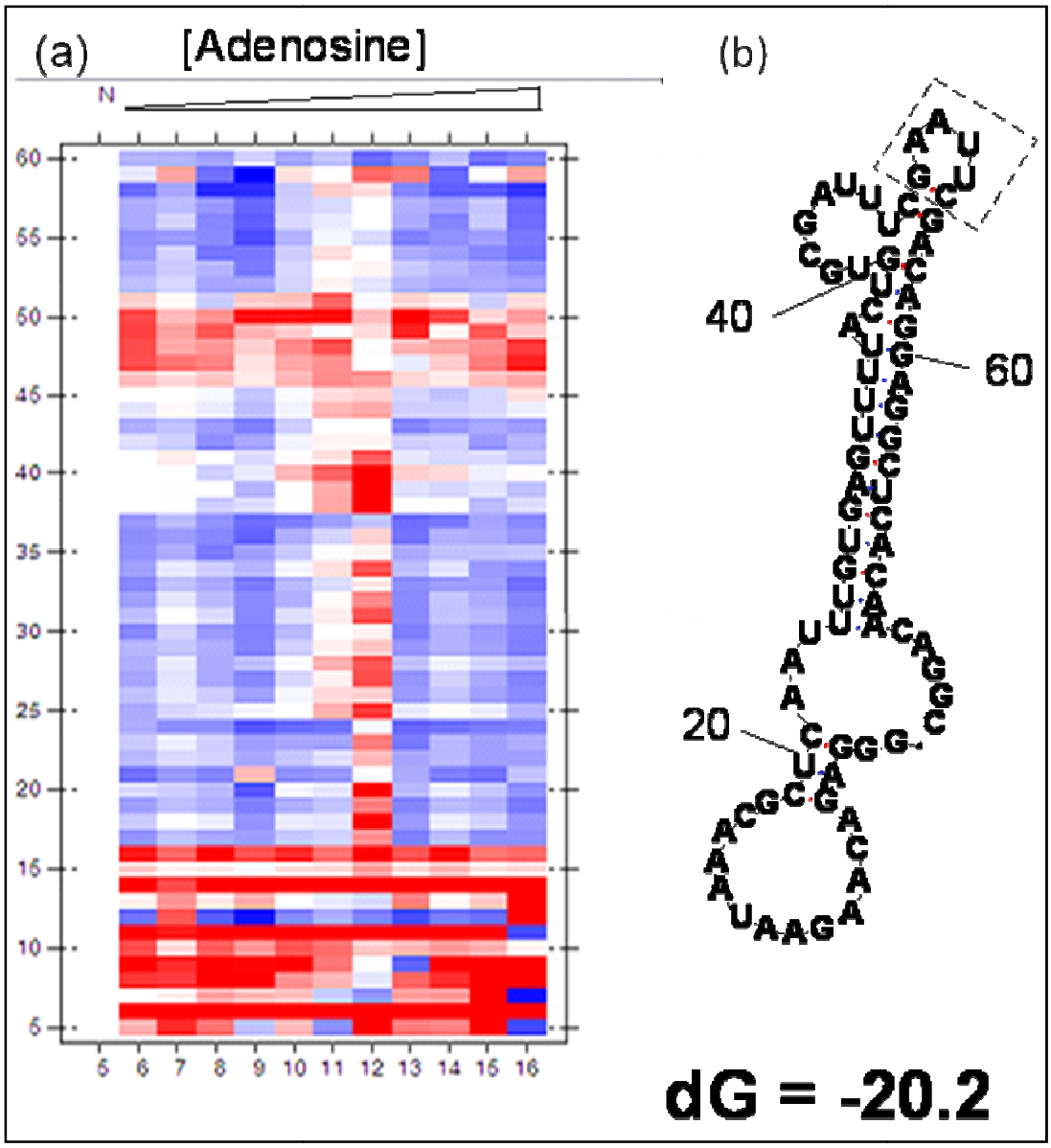

Figure 16: Enzymatic probing of S570.R14.C32 RNA pre-incubated with adenosine. (a) is the analyzed image using SAFA. The lanes that contained hydrolysate and the RNase T1 digest were removed from the analysis. The data were normalized such that undigested RNA equals zero. (b) one of the secondary structures that is consistent with the data obtained. The region of interest is indicated by dotted lines. (c) the raw gel image.

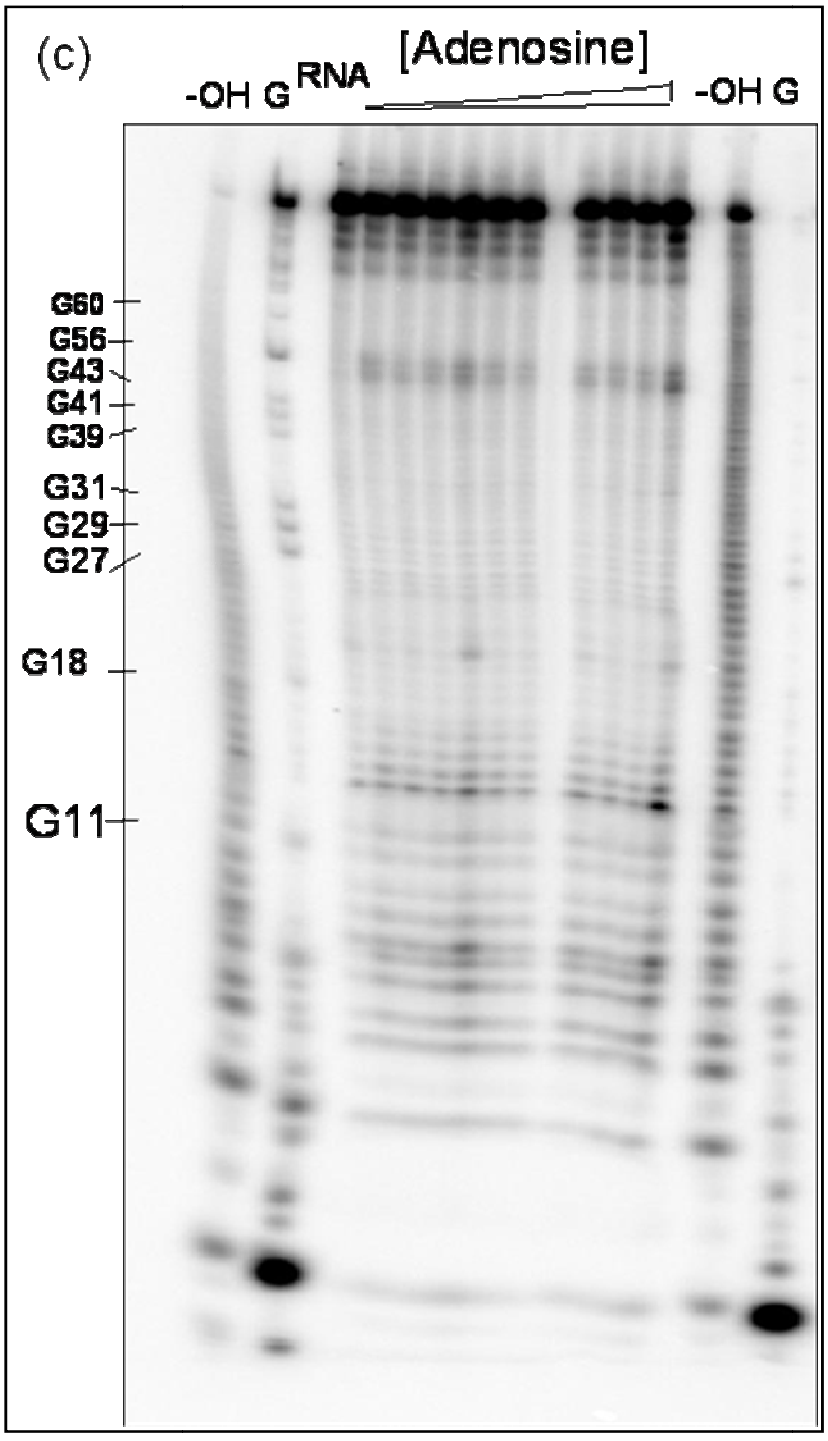

Figure 16: (continued)

The affinity of the S570.R14.C32T2 aptamer for PD173955N was determined by ITC in the buffer that mimics intracellular conditions (13.5 mM NaCl, 150 mM KCl, 220 µM Na_2HPO_4, 440 µM KH_2PO_4, 100 µM $MgSO_4$, 120 nM $CaCl_2$, 120 µM $MgCl_2$, 20 mM HEPES, 5% DMSO, pH 7.25) and in selection buffer (0.3 M KCl, 5 mM $MgCl_2$, 20 mM HEPES, 5% DMSO, pH 7.5). The S570.R14.C32RNA and S570.R14.C32T2 were found to have similar affinities for PD173955N (Figure 18, Page 67; Table 2, Page 49).

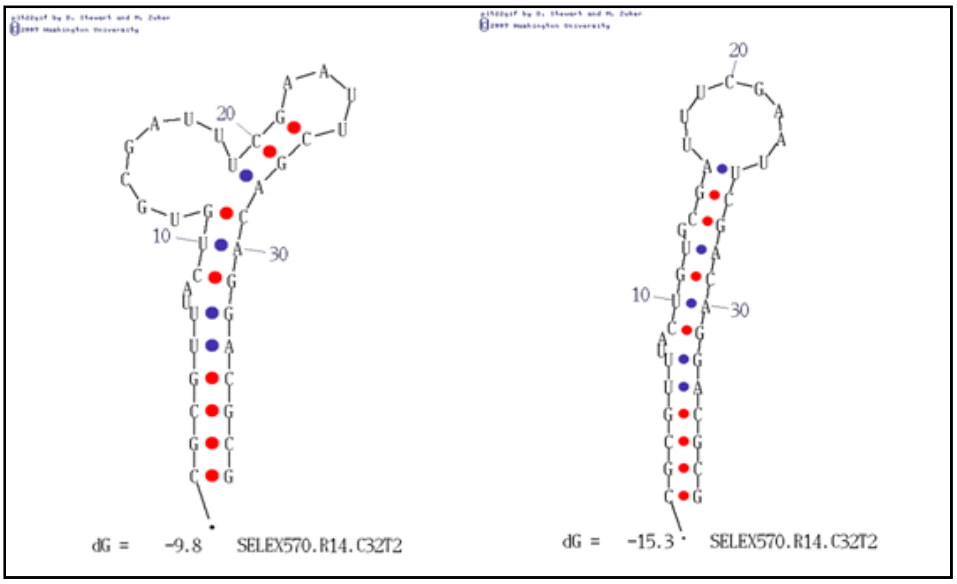

Figure 17: RNA secondary structures predicted by M-fold. Shown are the two most stable secondary structures of S570.R14.C32RNAT2 predicted by M-Fold.

In summary, these results show that the S570.R14.C32 contains an aptamer that recognizes PD173955N with high affinity, and that the region of the RNA responsible for binding PD173955N resides in the region represented by

S570.R14.c32T2 RNA. Thus, the portion of RNA that binds PD173955N was reduced from a 78mer to a 37mer.

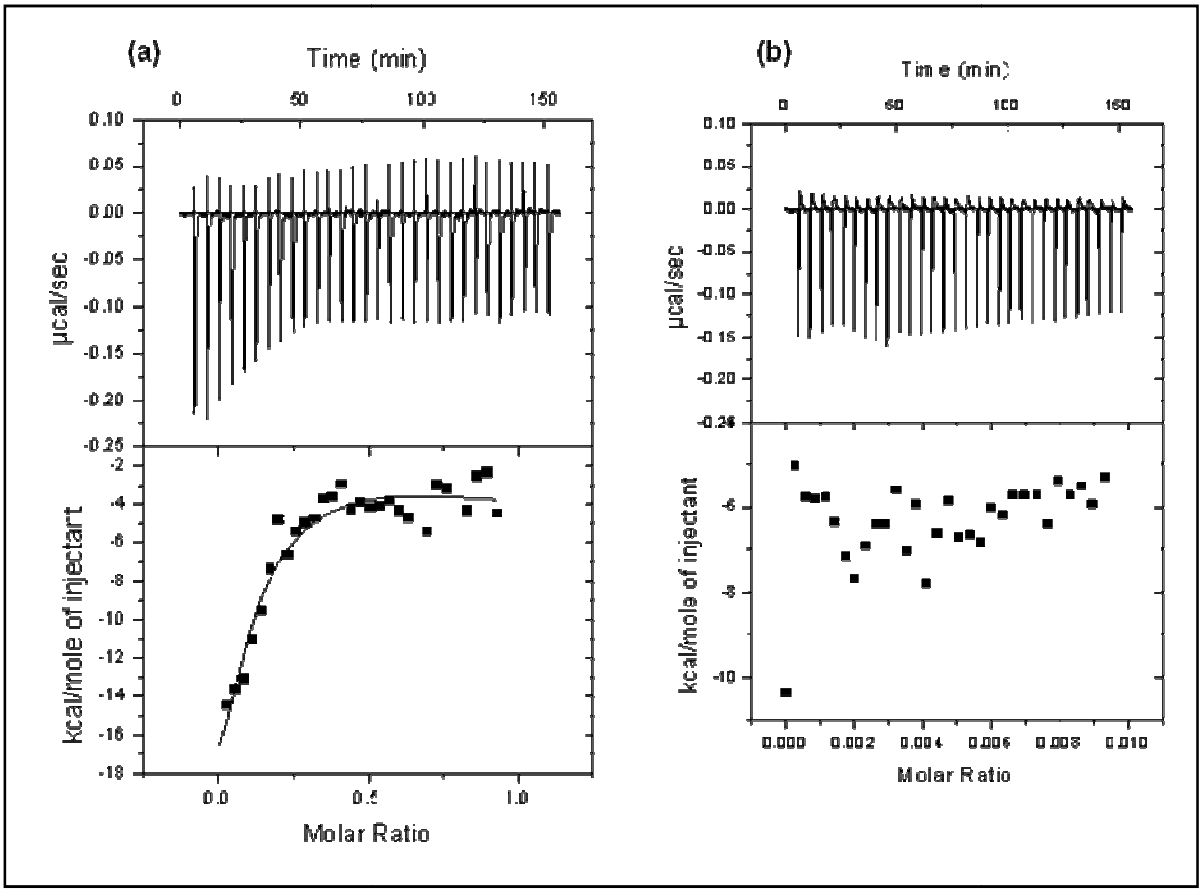

Figure 18: Determination of the thermodynamic parameters of S570.R14.C32T2 RNA aptamer by ITC. Shown is (a) the titration of 40 µM S570.R14.C32T2 RNA into a solution containing 10 µM PD173955N after the reference data was subtracted, (b) reference data with PD173955N titrated into the buffer. The K_D, calculated by the Origin software, is 1 µM. This experiment was repeated five times with similar results each time.

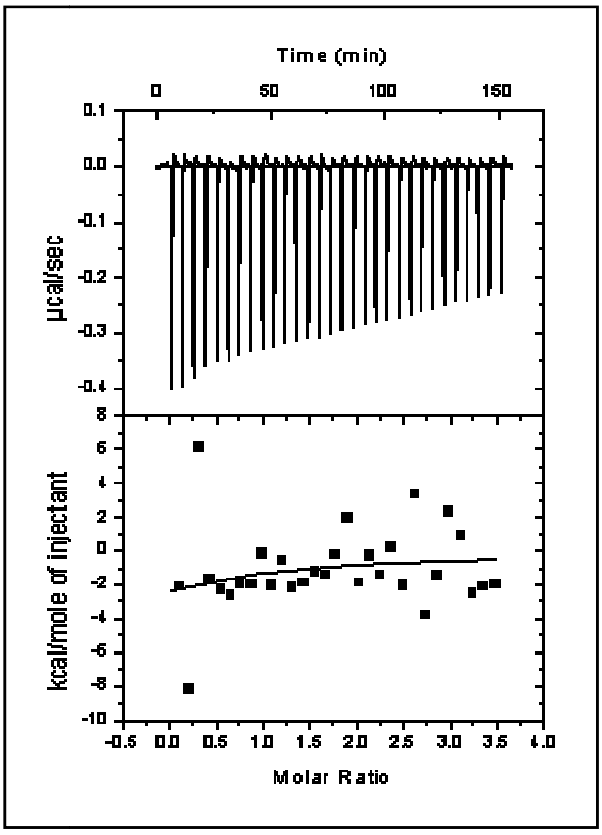

Figure 19: ITC titration of PD174265 with S570.R14.C32T2RNA. Shown is a titration of 75 µM PD174265 with 5 µM S570.R14.C32T2RNA in 300mM KCl, 20 mM HEPES, 5 mM $MgCl_2$, 5% DMSO pH 7.5 at 37°C after the data for PD174265 dilution into buffer was subtracted. The $K_{D,}$ calculated by the Origin software was 40 µM. However, the data does not show evidence of binding. This experiment was repeated two times with similar results each time.

CONCLUSION

The results presented here showed which part of the S570.R14.C32 RNA might be making contact with PD173955N, because incubation of the aptamer with PD173955N protected it from RNase ONE cleavage. Even though the use of RNase footprinting is time consuming, it can be used as an alternative method to determine binding affinities of the aptamers. Also it has been shown that reducing the size of

the aptamer in combination with addition of four GC pairs did not decrease the affinity of the aptamer. This means that, if necessary, other bases or even modified bases can be put on the end of the stem to make the selected aptamers more resistant to RNases *in vitro*. Further an increase in specificity and affinity of the truncated S570.r14.c32T2 aptamer can be achieved by doping the loop region where it is believed that the aptamer makes contact with PD173955N. Additional rounds of selection using the doped pool of aptamers would be necessary to do to get a more specific aptamer. The doping process involves synthesis of a random pool in which each position of the selected aptamer is mutated by a certain percentage. Doping would simplify the selection process and might give promising results. The RNA aptamer already binds the PD173955N and by doping not as many selection rounds would be necessary to select a higher affinity aptamer, compared with starting the SELEX experiment from beginning.

CHAPTER 4: GENERAL DISSCUSION AND RECOMMENDATIONS FOR FUTURE RESEARCH

Aptamers are becoming a prominent tool in many research areas. Their molecular properties make them more useful than antibodies for some applications. Development of the SELEX process made selection possible of rare nucleic acids to almost any target. As presented in this thesis the selection procedure does not yield an aptamer every time. The selection of aptamers is still very challenging, and needs more research to improve the efficiency of the selection procedure by finding methods to better capture RNA/target molecules. The results presented suggest that the use of the mathematical simulation modeling is beneficial, and can guide the set up SELEX experiments' starting conditions.

In Chapter two, the S570.R14.C32 RNA aptamer was selected to PD173955N with a dissociation constant between 1-2 μM. The same aptamer retained its binding affinity when it was used in buffer that mimics intracellular salt conditions. After the size of aptamer was reduced to the binding region, the affinity was not changed as shown in Chapter III. The high affinity toward PD173955N of the truncated aptamer may be because the nonbinding regions of the longer RNA interfered with aptamer folding in S570.R14.C32 RNA.

This aptamer was intended to be used to help increase the concentration of PD143955 inside cancerous leukemic cells. The affinity of the selected aptamer to the target may need to be improved for the proposed model to work and this can be achieved by partially randomizing (doping) the selected aptamer and continuing

SELEX for a few more rounds. This process is more promising than starting SELEX from the beginning. From this it is possible to generate an aptamer with higher affinity and specificity for PD173955.

As shown in the thesis, determining the aptamers' affinities was a very challenging task. PD173955N and PD173955B are very insoluble compounds and for use in ITC, high concentrations of the compounds were needed. The compounds were more soluble when DMSO was present in the binding reactions. The maximum solubility of PD173955N in selection buffer with 5% DMSO was 35 µM. It is unknown if 5% DMSO has any effect on the affinity of the RNA aptamer. Large concentrations of the RNA aptamers are needed for ITC experiments and they can be very costly. New methods to determine the binding constants of aptamers for small molecules need to be explored. ITC is a very reliable way to determine the binding constants, but for binding of low solubility small molecules is difficult to perform because it requires high concentrations of binding partners. Attaching the insoluble compounds to something more soluble like streptavidin might be a better way to determine the binding constant via ITC. Biotin labeled PD173955B can be attached to streptavidin and then concentrated down to get a highly concentrated sample that can be titrated into the cell compartment of the ITC machine containing the RNA aptamer. This would help reduce the cost associated with a generation of large amounts of RNA.

There are a number of usages for the selected aptamer. The selected aptamer can be attached to another aptamer like the PMSA aptamer, that

recognizes the PMSA protein present on the surface of prostate cancer cells, and be used to deliver PD173955N. The use of an aptamer to deliver drugs has already been proven to work, where the PMSA aptamer in conjugation with a nanoparticle was used to deliver hydrophilic and hydrophobic chemotherapeutic drugs to prostate cancer cells. The advantages of using aptamers over a nanoparticle are their smaller size that allows them to penetrate tissues faster. Another advantage is that they are biological molecules, and therefore are degradable to precursors that are not damaging to the cells. It would be ideal to take the S570.R14.C32 RNA aptamer, and create a 30% doped pool. Use of 2'-F-pyrimidines would allow generation of a more RNase resistant aptamer. The doped pool can be used to reselect again using PD173955B and substituting pyrimidines with 2'-F-pyrimidines. This selection would generate an aptamer that is more resistant to RNases and would increase its half life in blood.

REFERENCES

Biernaux, C., M. Loos, et al. (1995). "Detection of major bcr-abl gene expression at a very low level in blood cells of some healthy individuals." Blood **86**(8): 3118-3122.

Branford, S., Z. Rudzki, et al. (2003). "Detection of BCR-ABL mutations in patients with CML treated with imatinib is virtually always accompanied by clinical resistance, and mutations in the ATP phosphate-binding loop (P-loop) are associated with a poor prognosis." Blood **102**(1): 276-283.

Cox, J. C., A. Hayhurst, et al. (2002). "Automated selection of aptamers against protein targets translated in vitro: from gene to aptamer." Nucl. Acids Res. **30**(20): e108-.

Das, R., A. Laederach, et al. (2005). "SAFA: Semi-automated footprinting analysis software for high-throughput quantification of nucleic acid footprinting experiments." RNA **11**(3): 344-354.

Davis, K. A., Y. Lin, et al. (1998). "Staining of cell surface human CD4 with 2'-F-pyrimidine-containing RNA aptamers for flow cytometry." Nucl. Acids Res. **26**(17): 3915-3924.

Deininger, M. W. N., S. Bose, et al. (1998). "Selective Induction of Leukemia-associated Fusion Genes by High-Dose Ionizing Radiation." Cancer Res **58**(3): 421-425.

Dieckmann, T., E. Suzuki, et al. (1996). "Solution structure of an ATP-binding RNA aptamer reveals a novel fold." RNA **2**(7): 628-640.

Druker, B. J., C. L. Sawyers, et al. (2001). "Activity of a Specific Inhibitor of the BCR-ABL Tyrosine Kinase in the Blast Crisis of Chronic Myeloid Leukemia and Acute Lymphoblastic Leukemia with the Philadelphia Chromosome." N Engl J Med **344**(14): 1038-1042.

Ellington, A. D. and J. W. Szostak (1990). "In vitro selection of RNA molecules that bind specific ligands." Nature **346**(6287): 818-822.

Eulberg, D., K. Buchner, et al. (2005). "Development of an automated in vitro selection protocol to obtain RNA-based aptamers: identification of a biostable substance P antagonist." Nucl. Acids Res. **33**(4): e45-.

Floege, J., T. Ostendorf, et al. (1999). "Novel Approach to Specific Growth Factor Inhibition in Vivo : Antagonism of Platelet-Derived Growth Factor inGlomerulonephritis by Aptamers." Am J Pathol **154**(1): 169-179.

Fong, C.-t. and G. M. Brodeur (1987). "Down's syndrome and leukemia: Epidemiology, genetics, cytogenetics and mechanisms of leukemogenesis." Cancer Genetics and Cytogenetics **28**(1): 55-76.

Gambacorti-Passerini, C., R. Barni, et al. (2000). "Role of {alpha}1 Acid Glycoprotein in the In Vivo Resistance of Human BCR-ABL+ Leukemic Cells to the Abl Inhibitor STI571." J. Natl. Cancer Inst. **92**(20): 1641-1650.

Goldman, J. M. (2004). "Chronic myeloid leukemia--still a few questions." Experimental Hematology **32**(1): 2-10.

Gorre, M. E., M. Mohammed, et al. (2001). "Clinical Resistance to STI-571 Cancer Therapy Caused by BCR-ABL Gene Mutation or Amplification." Science **293**(5531): 876-880.

Green, L. S., D. Jellinek, et al. (1996). "Inhibitory DNA Ligands to Platelet-Derived Growth Factor B-Chain." Biochemistry **35**(45): 14413-14424.

Griffin, L. C., G. F. Tidmarsh, et al. (1993). "In vivo anticoagulant properties of a novel nucleotide-based thrombin inhibitor and demonstration of regional anticoagulation in extracorporeal circuits." Blood **81**(12): 3271-3276.

Hamada, A., H. Miyano, et al. (2003). "Interaction of Imatinib Mesilate with Human P-Glycoprotein." J Pharmacol Exp Ther **307**(2): 824-828.

Hamby, J. M., C. J. C. Connolly, et al. (1997). "Structure-Activity Relationships for a Novel Series of Pyrido[2,3-d]pyrimidine Tyrosine Kinase Inhibitors." J. Med. Chem. **40**(15): 2296-2303.

Hamula, C. L. A., J. W. Guthrie, et al. (2006). "Selection and analytical applications of aptamers." TrAC Trends in Analytical Chemistry **25**(7): 681-691.

Hauptmann, M., J. H. Lubin, et al. (2003). "Mortality From Lymphohematopoietic Malignancies Among Workers in Formaldehyde Industries." J. Natl. Cancer Inst. **95**(21): 1615-1623.

John, M. G. (2003). "Chronic myeloid leukemia-still a few questions." Experimental hematology **32**(1): 2-10.

Kim, M. Y. and S. Jeong (2004). "Inhibition of the functions of the nucleocapsid protein of human immunodeficiency virus-1 by an RNA aptamer." Biochemical and Biophysical Research Communications **320**(4): 1181-1186.

Kurzrock, R., H. M. Kantarjian, et al. (2003). "Philadelphia Chromosome-Positive Leukemias: From Basic Mechanisms to Molecular Therapeutics." Ann Intern Med **138**(10): 819-830.

le Coutre, P., E. Tassi, et al. (2000). "Induction of resistance to the Abelson inhibitor STI571 in human leukemic cells through gene amplification." Blood **95**(5): 1758-1766.

Levine, H. A. and M. Nilsen-Hamilton (2007). "A mathematical analysis of SELEX." Computational Biology and Chemistry **31**(1): 11-35.

Liangfang Zhang, Aleksandar F. R.-M. F. A. Frank X. G. Pamela A. B. V. B. S. J. Robert S. L. Omid C. F. (2007). "Co-Delivery of Hydrophobic and Hydrophilic Drugs from Nanoparticle-Aptamer Bioconjugates." ChemMedChem **9999**(9999): NA.

Lugo, T. G., A. M. Pendergast, et al. (1990). "Tyrosine kinase activity and transformation potency of bcr-abl oncogene products." Science **247**(4946): 1079-1082.

McWhirter, J. R., D. L. Galasso, et al. (1993). "A coiled-coil oligomerization domain of Bcr is essential for the transforming function of Bcr-Abl oncoproteins." Mol. Cell. Biol. **13**(12): 7587-7595.

Mesa, R. A., M. A. Elliott, et al. (2000). "Splenectomy in chronic myeloid leukemia and myelofibrosis with myeloid metaplasia." Blood Reviews **14**(3): 121-129.

Moasser, M. M., M. Srethapakdi, et al. (1999). "Inhibition of Src Kinases by a Selective Tyrosine Kinase Inhibitor Causes Mitotic Arrest." Cancer Res **59**(24): 6145-6152.

Murphy, M. B., S. T. Fuller, et al. (2003). "An improved method for the in vitro evolution of aptamers and applications in protein detection and purification." Nucl. Acids Res. **31**(18): e110-.

Nagar, B., W. G. Bornmann, et al. (2002). "Crystal Structures of the Kinase Domain of c-Abl in Complex with the Small Molecule Inhibitors PD173955 and Imatinib (STI-571)." Cancer Res **62**(15): 4236-4243.

Nagar, B., O. Hantschel, et al. (2003). "Structural Basis for the Autoinhibition of c-Abl Tyrosine Kinase." Cell **112**(6): 859-871.

Ng, E. W. M., D. T. Shima, et al. (2006). "Pegaptanib, a targeted anti-VEGF aptamer for ocular vascular disease." Nat Rev Drug Discov **5**(2): 123-132.

Pendergrast, P. S., H. N. Marsh, et al. (2005). "Nucleic Acid Aptamers for Target Validation and Therapeutic Applications." J Biomol Tech **16**(3): 224-234.

Pietras, K., K. Rubin, et al. (2002). "Inhibition of PDGF Receptor Signaling in Tumor Stroma Enhances Antitumor Effect of Chemotherapy." Cancer Res **62**(19): 5476-5484.

Proske, D., M. Blank, et al. (2005). "Aptamers—basic research, drug development, and clinical applications." Applied Microbiology and Biotechnology **69**(4): 367-374.

Ring, H. Z. and J. T. Lis (1994). "The SR protein B52/SRp55 is essential for Drosophila development." Mol. Cell. Biol. **14**(11): 7499-7506.

Sassanfar, M. and J. W. Szostak (1993). "An RNA motif that binds ATP." Nature **364**(6437): 550-553.

Sayer, N., J. Ibrahim, et al. (2002). "Structural characterization of a 2'F-RNA aptamer that binds a HIV-1 SU glycoprotein, gp120." Biochemical and Biophysical Research Communications **293**(3): 924-931.

Sazani, P. L., R. Larralde, et al. (2004). "A Small Aptamer with Strong and Specific Recognition of the Triphosphate of ATP." J. Am. Chem. Soc. **126**(27): 8370-8371.

Shi, H., B. E. Hoffman, et al. (1999). "RNA aptamers as effective protein antagonists in a multicellular organism." PNAS **96**(18): 10033-10038.

Shuryak, I., R. K. Sachs, et al. (2006). "Radiation-Induced Leukemia at Doses Relevant to Radiation Therapy: Modeling Mechanisms and Estimating Risks." J. Natl. Cancer Inst. **98**(24): 1794-1806.

Smith, M. T. (1996). "The mechanism of benzene-induced leukemia: a hypothesis and speculations on the causes of leukemia." Environmental Health Perspectives **104**: 1219-1225.

Society, A. C. (2007). "Cancer Facts and Figures 2007." American Cancer Society.

Talpaz, M., N. P. Shah, et al. (2006). "Dasatinib in Imatinib-Resistant Philadelphia Chromosome-Positive Leukemias." N Engl J Med **354**(24): 2531-2541.

Talpaz, M., R. T. Silver, et al. (2002). "Imatinib induces durable hematologic and cytogenetic responses in patients with accelerated phase chronic myeloid leukemia: results of a phase 2 study." Blood **99**(6): 1928-1937.

Tucker, M. A., A. T. Meadows, et al. (1987). "Leukemia after therapy with alkylating agents for childhood cancer." J. Natl. Cancer Inst. ; Vol/Issue: 3: Pages: 459-464.

Tuerk, C. and L. Gold (1990). "Systematic evolution of ligands by exponential enrichment: RNA ligands to bacteriophage T4 DNA polymerase." Science **249**(4968): 505-510.

Tulasne, D., B. A. Judd, et al. (2001). "C-terminal peptide of thrombospondin-1 induces platelet aggregation through the Fc receptor gamma -chain-associated signaling pathway and by agglutination." Blood **98**(12): 3346-3352.

Vaish, N. K., R. Larralde, et al. (2003). "A Novel, Modification-Dependent ATP-Binding Aptamer Selected from an RNA Library Incorporating a Cationic Functionality." Biochemistry **42**(29): 8842-8851.

Van Etten, R. A. (1999). "Cycling, stressed-out and nervous: cellular functions of c-Abl." Trends in Cell Biology **9**(5): 179-186.

Weisberg, E. and J. D. Griffin (2000). "Mechanism of resistance to the ABL tyrosine kinase inhibitor STI571 in BCR/ABL-transformed hematopoietic cell lines." Blood **95**(11): 3498-3505.

Wisniewski, D., C. L. Lambek, et al. (2002). "Characterization of Potent Inhibitors of the Bcr-Abl and the c-Kit Receptor Tyrosine Kinases." Cancer Res **62**(15): 4244-4255.

Wissing, J., K. Godl, et al. (2004). "Chemical Proteomic Analysis Reveals Alternative Modes of Action for Pyrido[2,3-d]pyrimidine Kinase Inhibitors." Mol Cell Proteomics **3**(12): 1181-1193.